

Computational Science

An Industrial Perspective Workshop

**Multiscale Modeling for the Development of
Commercial Materials and Devices**

Dr. Edward Furlani

**Dept. of Chemical and Biological Engineering
Dept. Electrical Engineering**

Interdisciplinary Computational Research

Academic Research: SUNY at Buffalo (2011 - present)

Prof. Chemical and Biological Engineering

Prof. Electrical Engineering



Dr. Edward Furlani
[\(efurlani@buffalo.edu\)](mailto:efurlani@buffalo.edu)

Industrial Research: Eastman Kodak Research Labs (1982 – 2010)
Computational modeling for commercial product development.

Research Areas

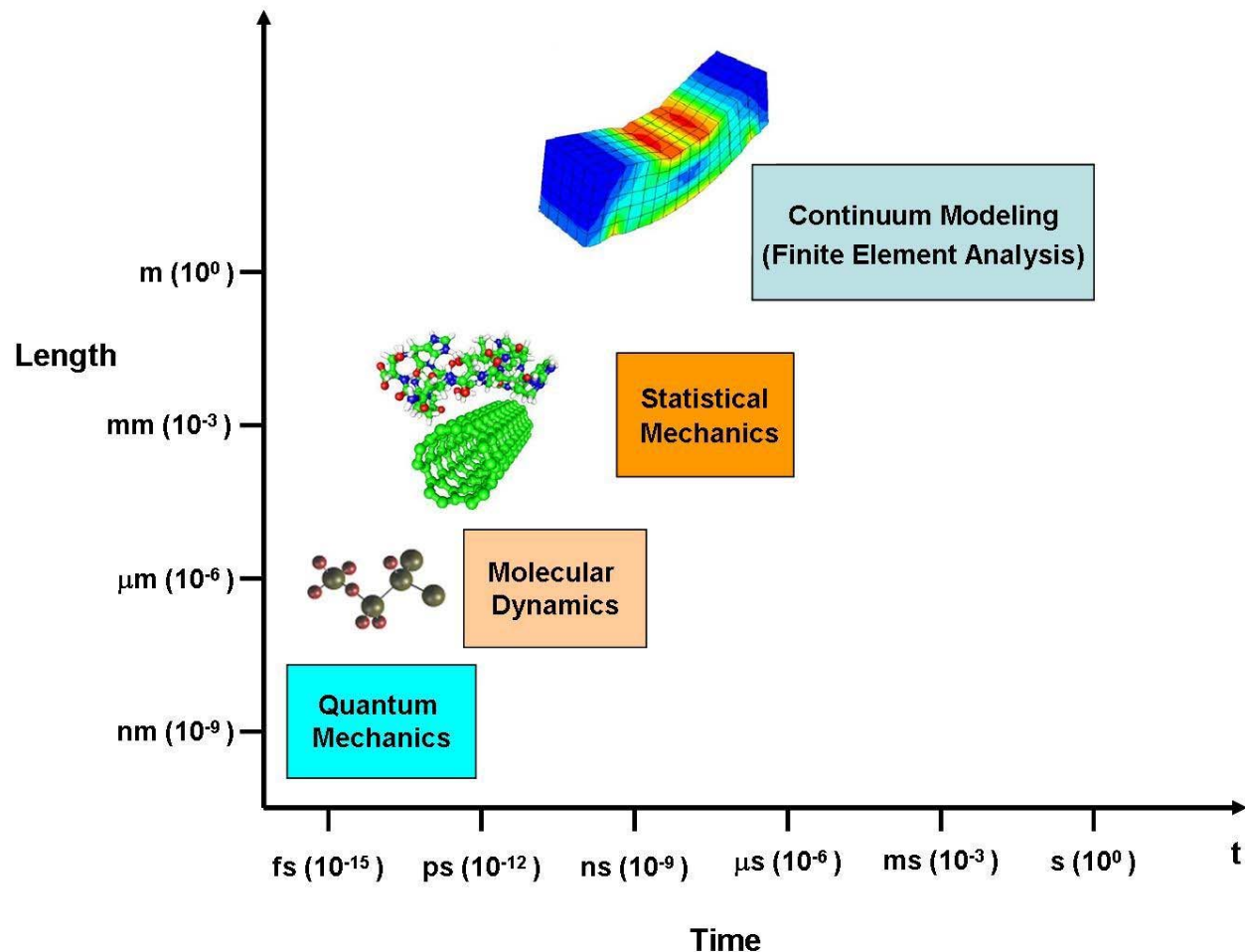
- Nanophotonics: plasmonics, photothermal phenomena, metamaterials
- Computational fluid dynamics (CFD): multiphase systems, heat/mass transfer, nanofluids, ink jet systems
- Microfluidics: devices and processes, design and simulation
- Computational Magnetics: Directed self-assembly, bioseparation, drug delivery
- MOEMS/MEMS: design and simulation

Presentation Overview

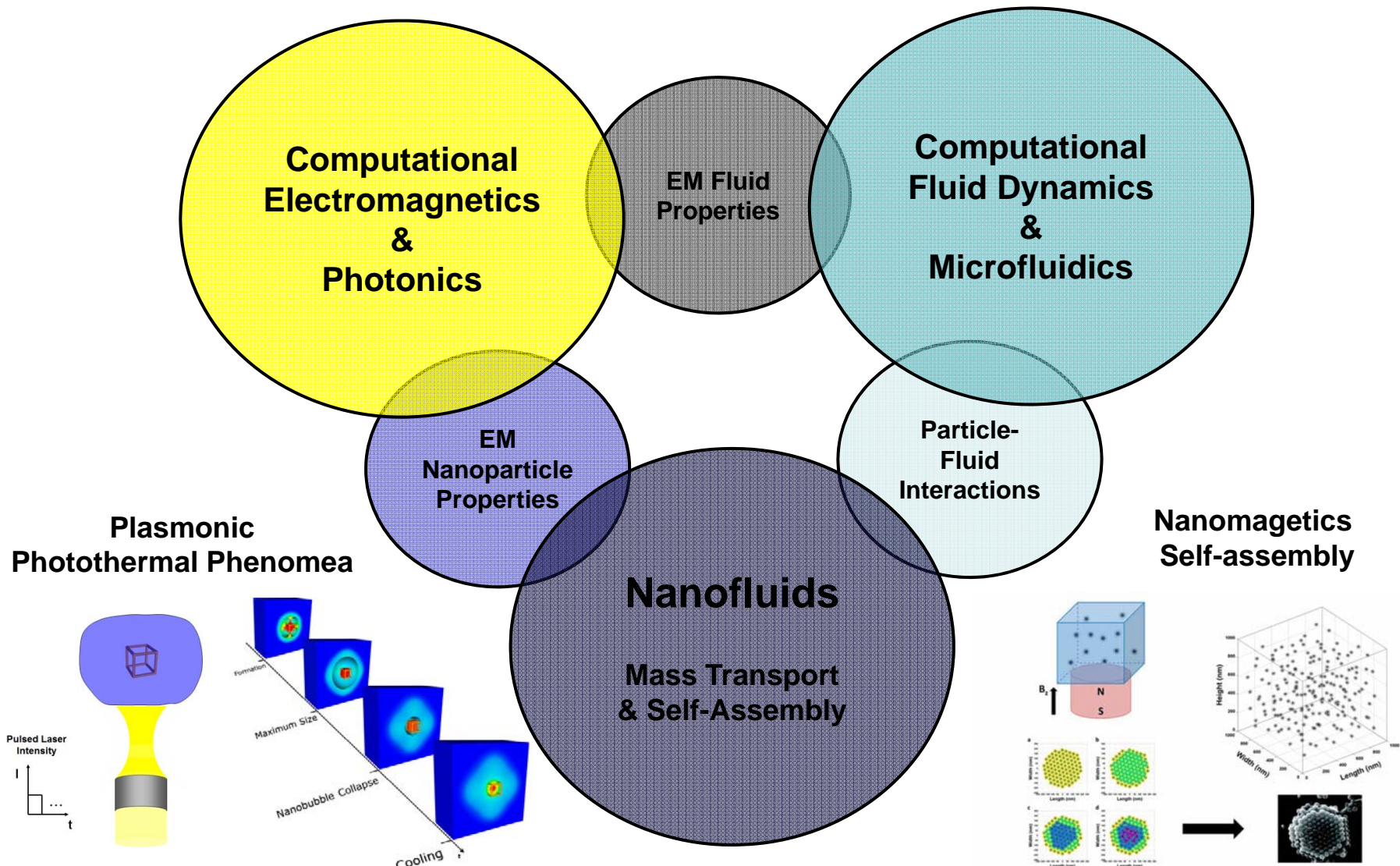
- **Introduction**
 - Modeling Overview
 - Kodak Materials and Micro-Device Research
- **Micro-Optical Electro-Mechanical Devices**
- **Microfluidics: Inkjet Technology**
- **Summary**

Multiscale Modeling

Modeling Phenomena Across Multiple Length and Time Scales

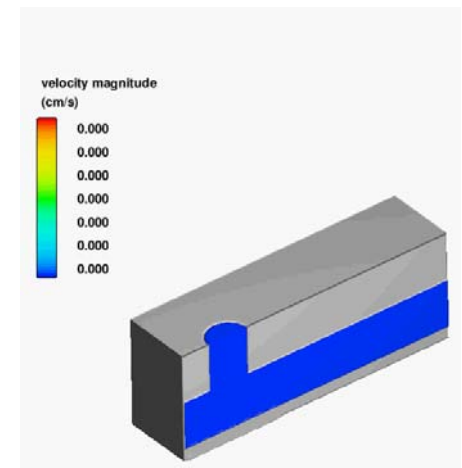


Interdisciplinary Computational Research

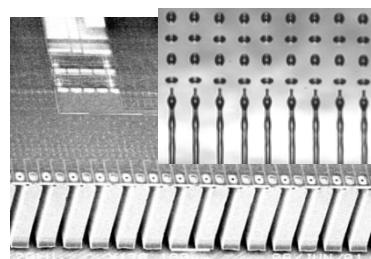


Modeling Overview

Inkjet Printing



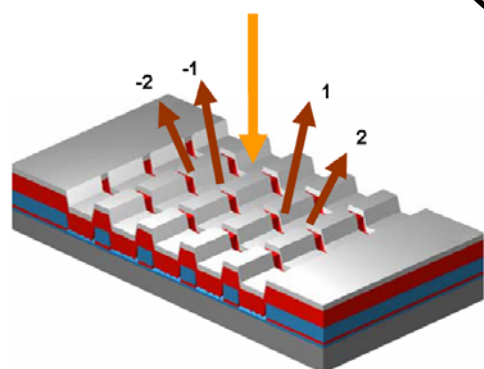
Inkjet Printing



Micro Nozzle Array

Microfluidics
InkJet

MEMS
Light Modulator

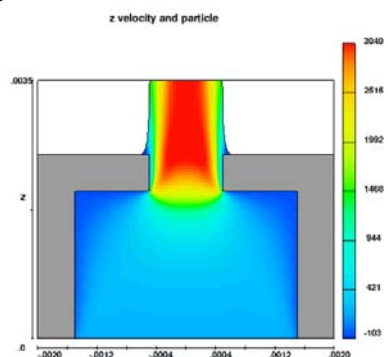


Micro-Optical
Electro-Mechanical
Devices

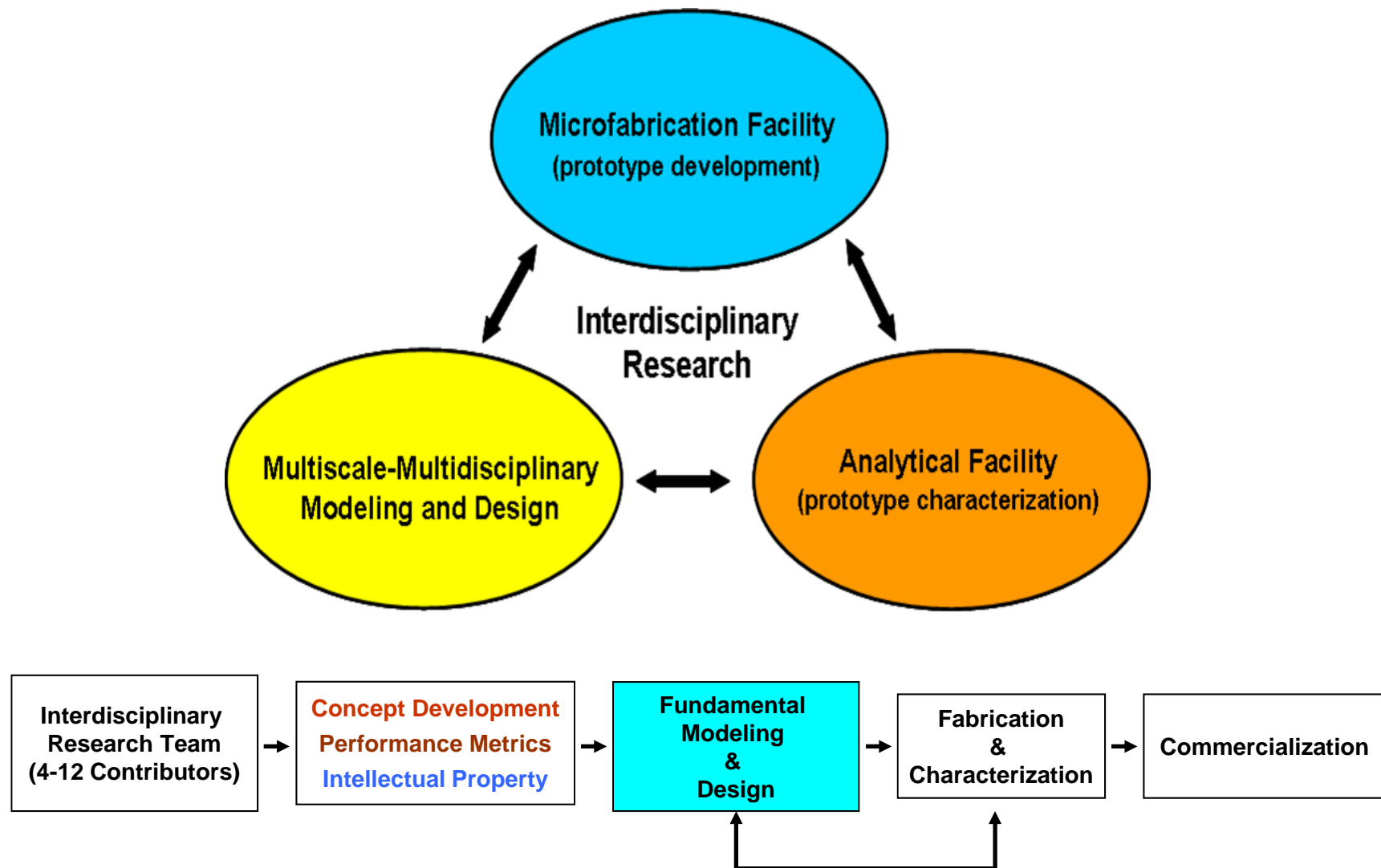
Nanofluids
Mass Transport

Nanofluids

Pigment 60 nm



Kodak Materials & Microdevice Research



Materials & Microdevice Research

In House Prototype Development Facility

12,000 sq ft Class 100/1000 Clean Room

- Processing: 6" (150mm) Si wafers
- Resolution: 0.5µm features
- Full CMOS* Integration

- Clean/Wet Etch
 - Megasonics cleaner
 - Spin spray rinser/dryer
- Deposition
 - CVC sputterer
 - LPCVD furnace
 - PEO annealing furnace
- Lithography
 - Canon stepper
 - Spin coater
 - Polyimide/PMDS ovens
- Dry Etch
 - Oxford etcher
 - Dielectric Etch
- STS
 - STS cluster tool
 - Wafer grinder
- Analytical
 - Ellipsometer
 - Reflectrometer
 - SEM
 - Profilometer

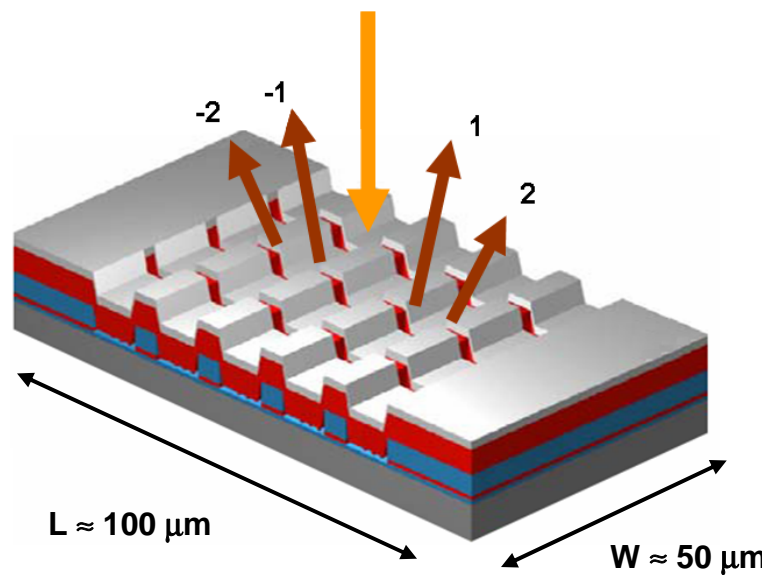


*CMOS = Complementary Metal–Oxide–Semiconductor

Micro-Optical Electro-Mechanical Devices

Kodak MEMS Light Modulator

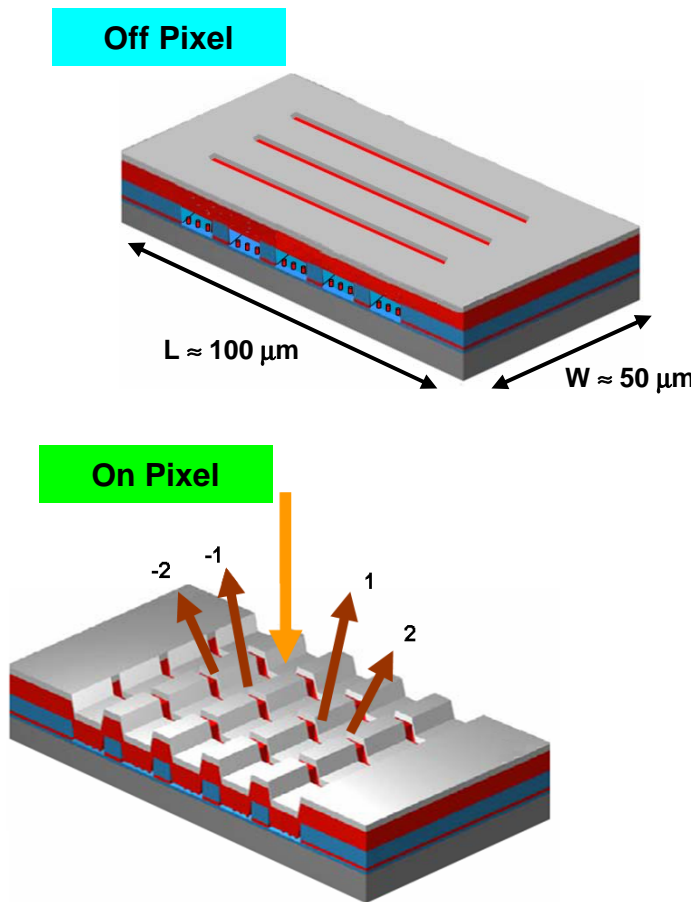
Micromachined Reflection Grating



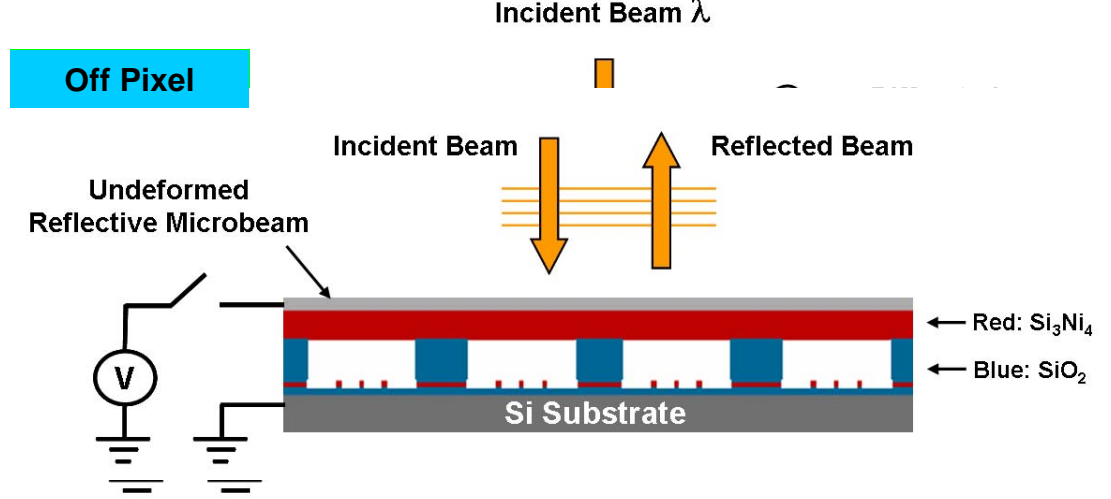
Motivation: Solid State Display Applications

Micro-Optical Electro-Mechanical Analysis

Modeling and Device Design

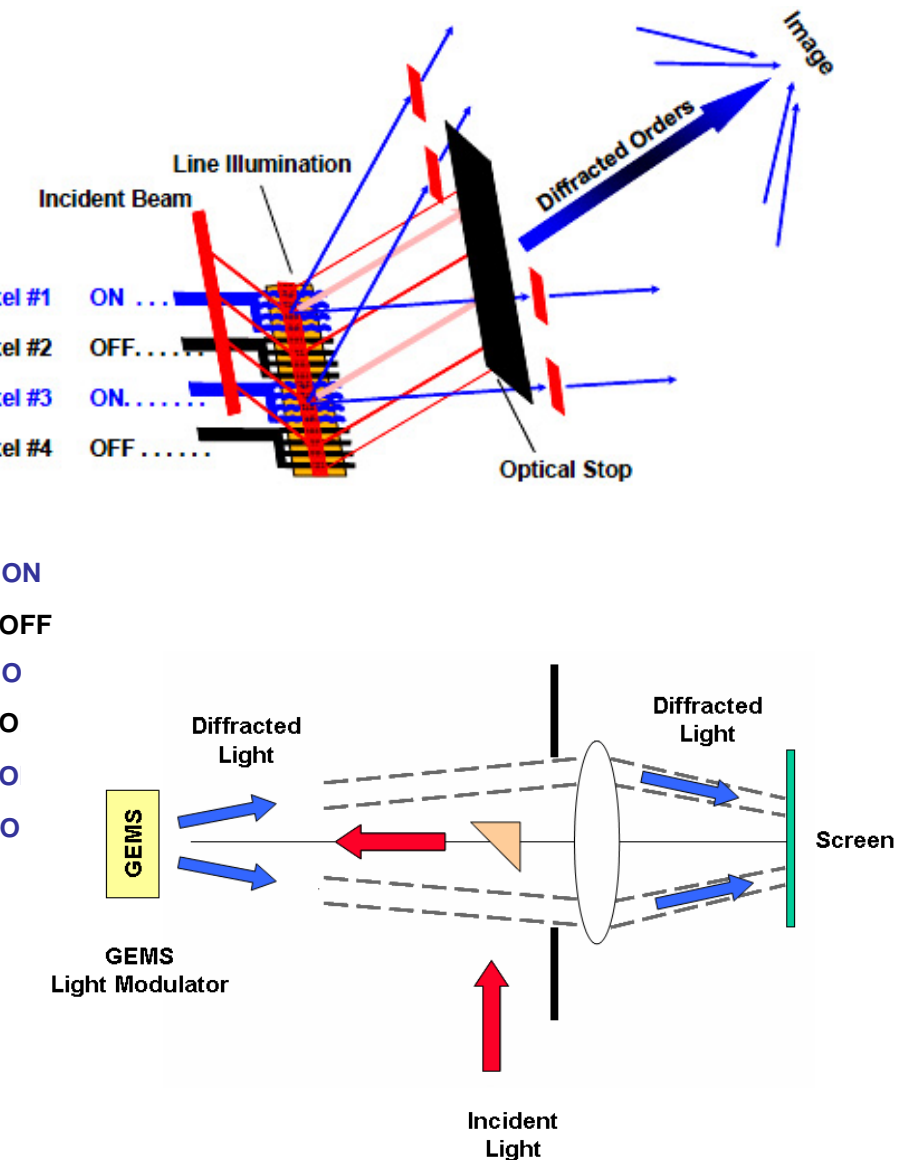
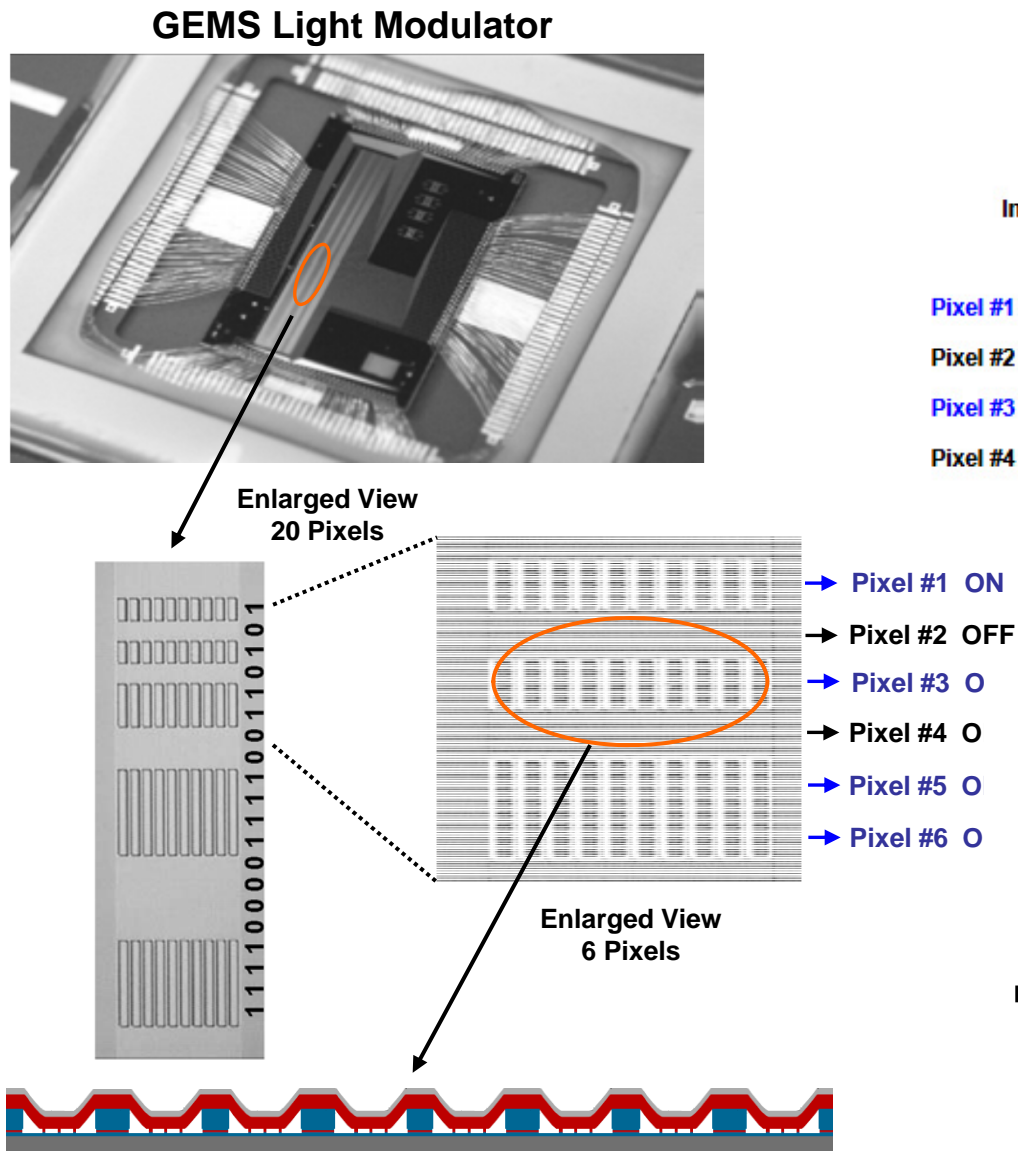


**Kodak GEMS* Technology
(Grating Electromechanical System)**



*M. Kowarz, *Spatial light modulator with conformal grating device*, US. Patent 6307663, 2001.

Display Applications: Linear Array Operation



Commercial Projection Display

Front Projection System

Applications

- Front projection Systems
- Rear projection laser TV
- Heads-up displays
- Laser Printing

The diagram illustrates the optical path of a front projection system. Three laser beams—Red (R), Green (G), and Blue (B)—each pass through a GEMS (Galvanometer Electro-Mechanical Scanner) component. The Red beam is directed upwards by a mirror, while the Green and Blue beams are directed downwards. These three beams converge at an X-cube, which then directs them to a Galvanometer Mirror. The Galvanometer Mirror reflects the beams onto a Projection Lens, which focuses the light onto a screen. The diagram also shows a Patterned Turning Mirror and another GEMS component.

Photograph of Scene from Scanned Motion Picture Film

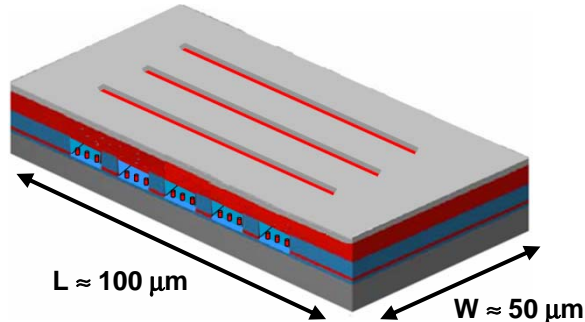
A photograph showing a scene from a scanned motion picture film. Two women are smiling; one is wearing a green cap and the other is wearing a pink shirt. They are holding a tray filled with oranges. The image is displayed on a front projection screen.

115 in Front Projection Display

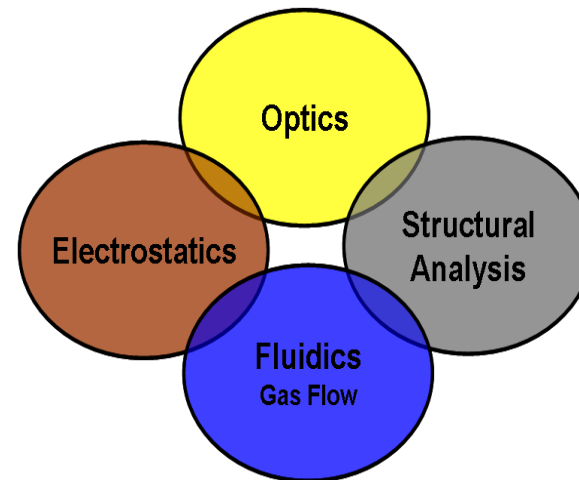
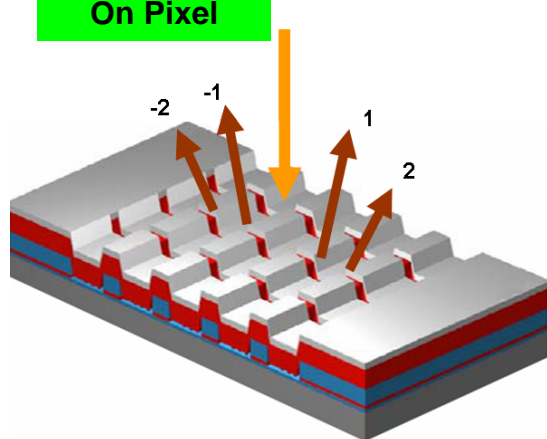
A photograph of the internal mechanical components of a front projection display. The image shows various optical elements and electronic components. Labels point to specific parts: GEMS (Galvanometer Electro-Mechanical Scanner), Galvanometer Mirror, X-cube, and another GEMS component. A large black arrow points from the top diagram towards this photograph.

Device Analysis and Rational Design

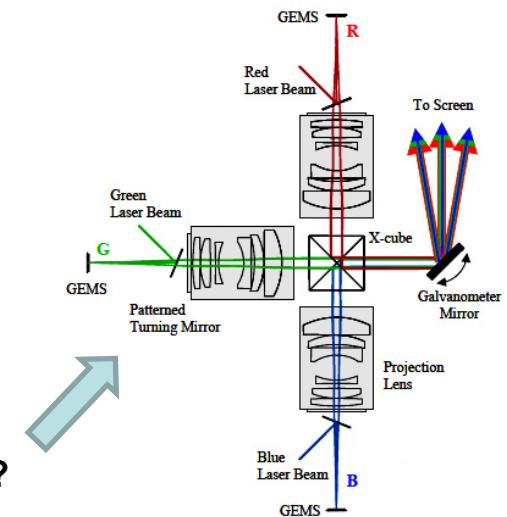
Off Pixel



On Pixel



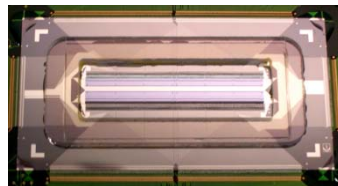
- Operating Voltage?
- Microbeam Deformation Profile?
- Diffraction Efficiency?
- Dynamic Response of Microbeam?



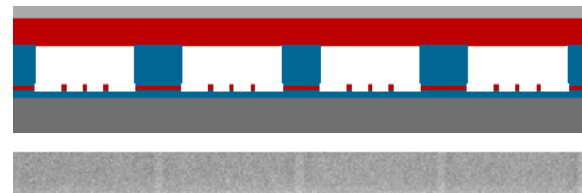
Length and Time Scales

Length

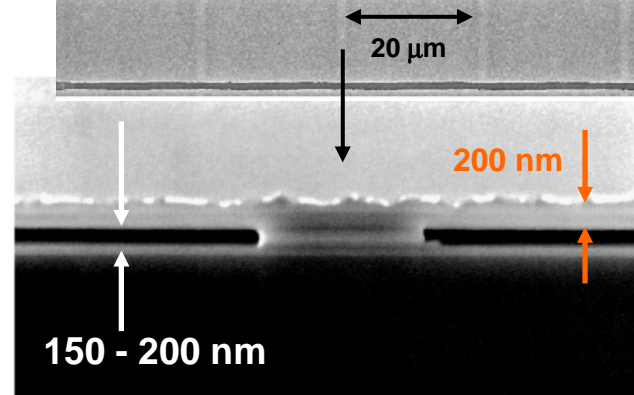
Mesoscale (mm)



Microscale



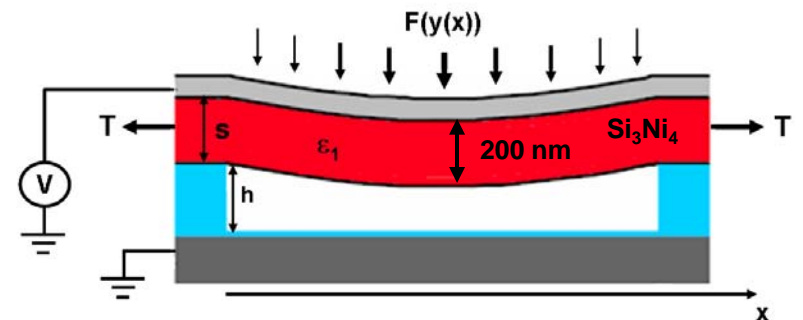
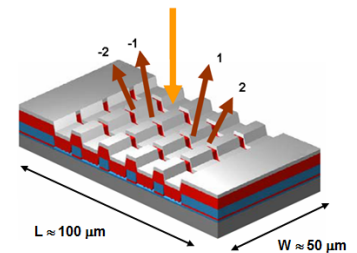
Nanoscale



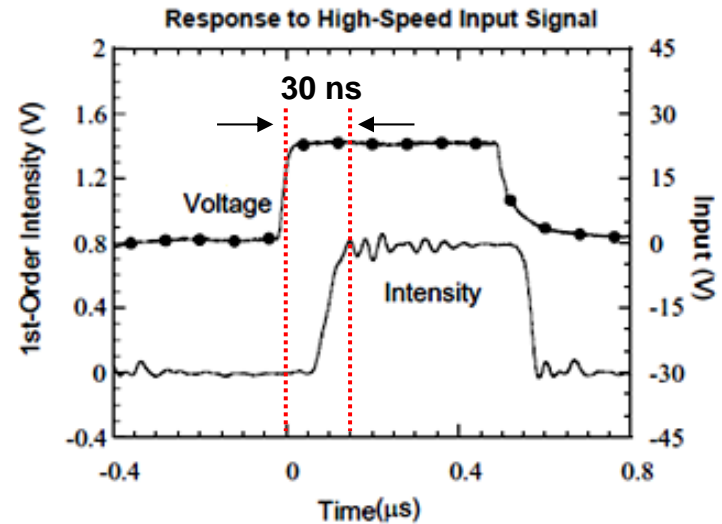
SEM: Gap Beneath Microbeam

Mean free path of air molecules
beneath microbeam = 65 nm!

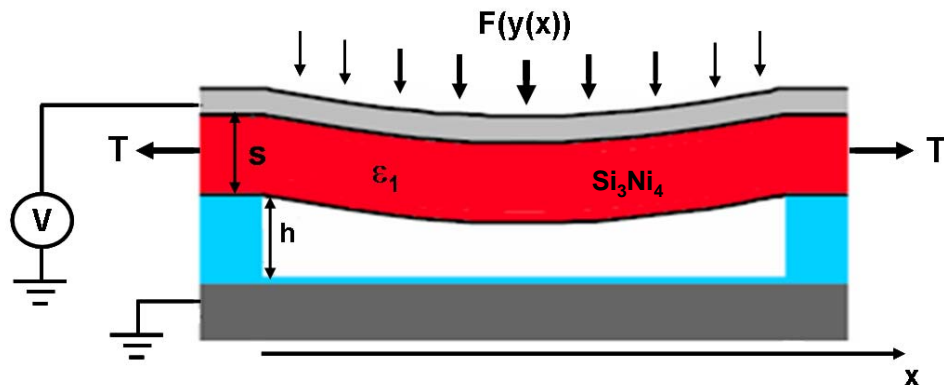
Time



Microbeam Response Time = 30 ns



Electrostatic Deformation of Microbeam



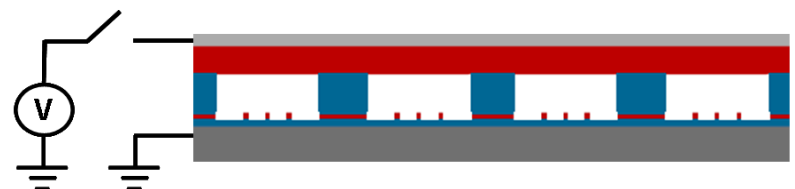
Predict
Deformation Profile vs. Activation Voltage

$$\underbrace{EI \frac{d^4 y}{dx^4}}_{\text{Bending}} - \underbrace{T \frac{d^2 y}{dx^2}}_{\text{Tension}} = \underbrace{f_e(y)}_{\text{Electrostatic Force per Length}}$$

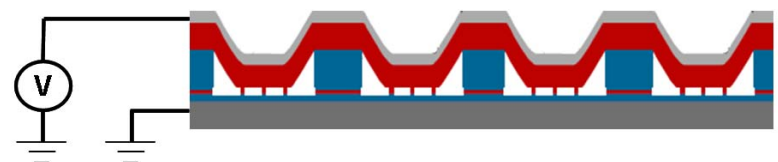
Nonlinear Electrostatic Force per Length

$$f_e(y) = \frac{\epsilon_1^2 \epsilon_0 w}{2} \frac{V^2}{[\epsilon_0 s + \epsilon_1(h-y)]^2}$$

T = Tensile Force in Si_3Ni_4
 E = Young's Modulus
 I = Moment of Inertia

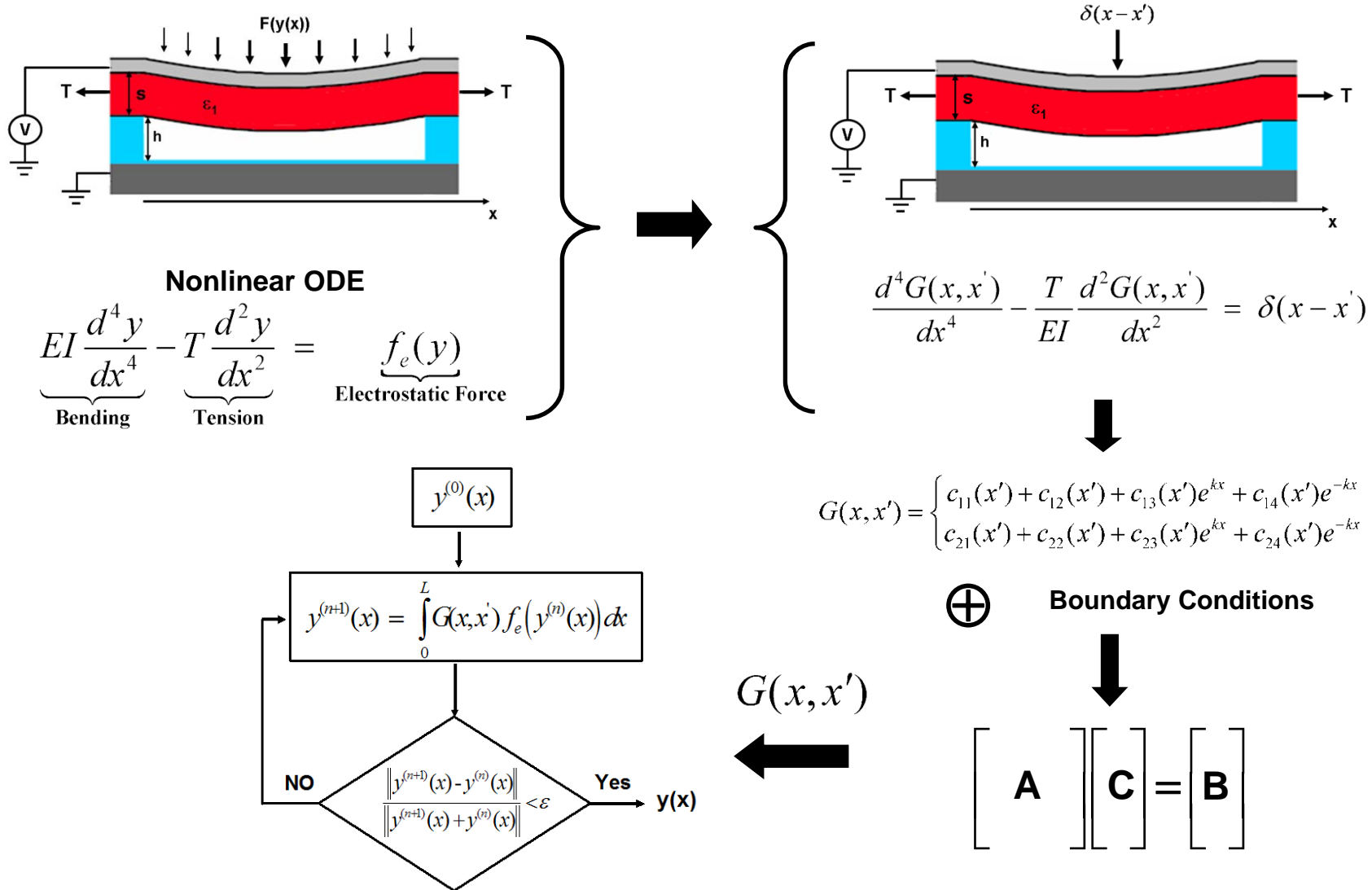


Pull-In Voltage



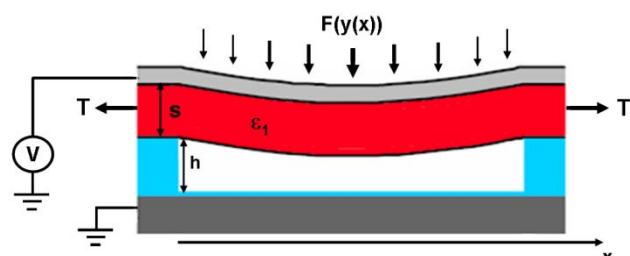
Predict Deformation of Microbeam

Self-Consistent Green's Function Analysis*



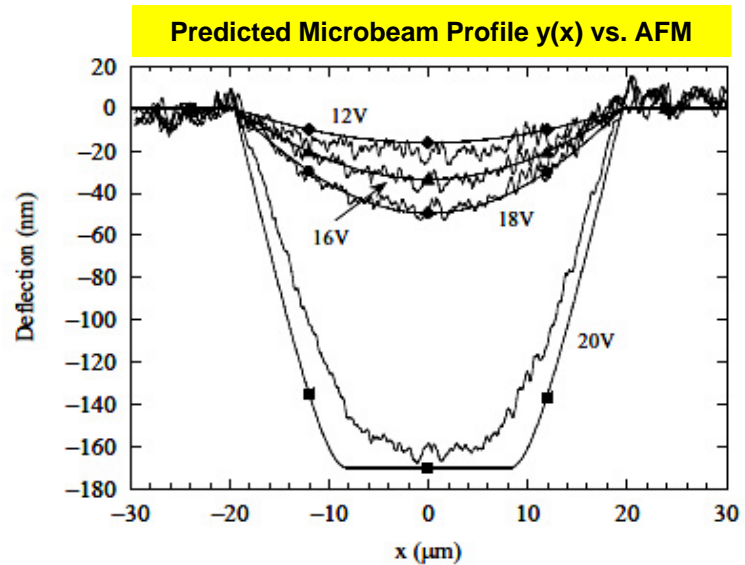
*E. P. Furlani, *Analysis of grating light valves with partial surface electrodes*, J. Appl. Phys. 83 1998.

Microbeam Deformation: Model vs. Experiment



$$\underbrace{EI \frac{d^4 y}{dx^4}}_{\text{Bending}} - \underbrace{T \frac{d^2 y}{dx^2}}_{\text{Tension}} = \underbrace{f_e(y)}_{\text{Electrostatic Force}}$$

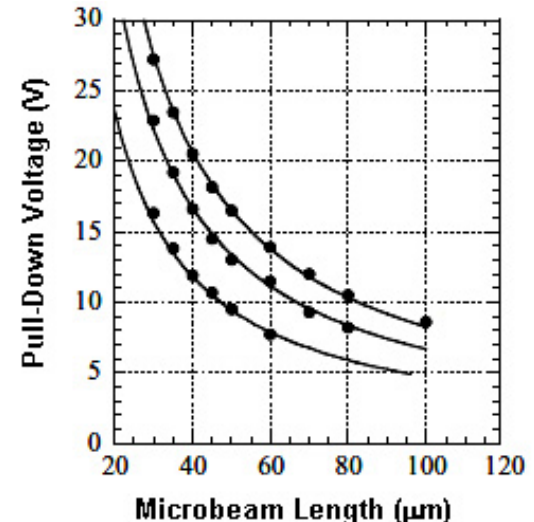
$y(x)$



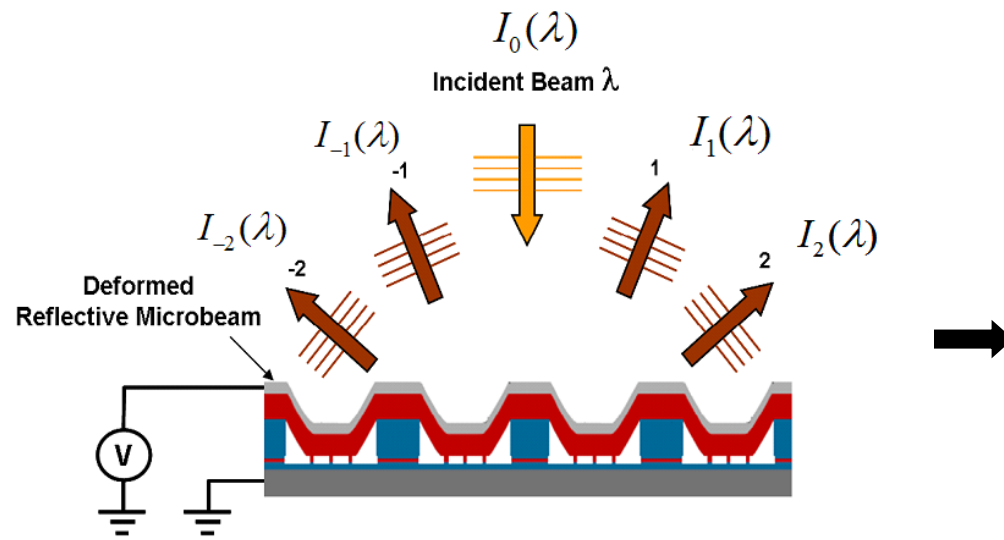
Activation Voltage: Theory vs. Experiment

Tensile Stress T [MPa]	Beam Length L [μm]	Switching Voltage, V_2	
		Measured V_2 [V]	Theoretical V_2 [V]
800	20	18	18.6
800	16	26	23.4
400	16	18	17.0
100	16	11	9.6

Optimization



Optical Diffraction Efficiency



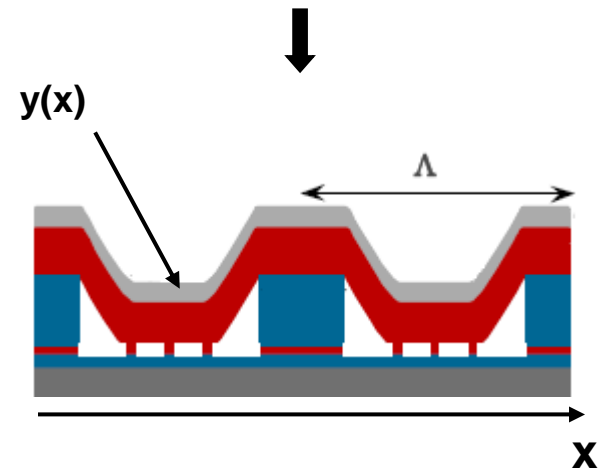
Trapezoidal Microbeam Profile

$$\eta_m = \frac{64h^2}{m^2\pi^2\lambda^2} \left[\frac{m\left(1 - \frac{2b}{\Lambda}\right)\cos\left(\frac{m\pi b}{\pi}\right)\sin\left(\frac{2\pi h}{\lambda} - \frac{m\pi}{2}\right)}{m^2\left(1 - \frac{2b}{\Lambda}\right)^2 - \frac{16h^2}{\lambda^2}} + \frac{\sin\left(\frac{m\pi b}{\pi}\right)\cos\left(\frac{2\pi h}{\lambda} - \frac{m\pi}{2}\right)}{m^2\left(1 - \frac{2b}{\Lambda}\right)^2 - \frac{16h^2}{\lambda^2}} \right]$$

Scalar Diffraction Theory

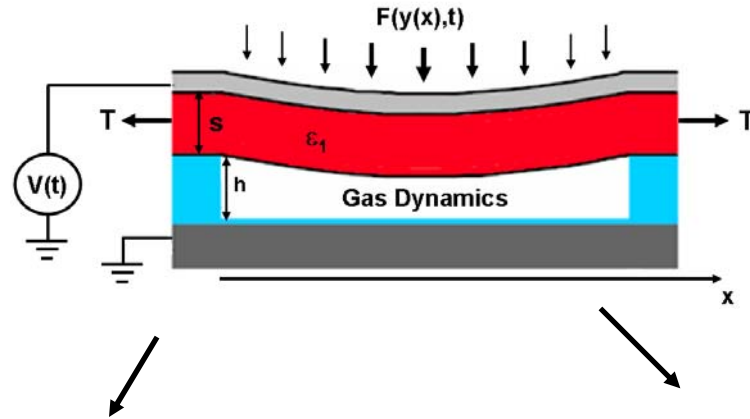
$$I_m(\lambda) = I_0(\lambda)\eta_m$$

$$\eta_m = \left| \frac{1}{\Lambda} \int_0^\Lambda e^{i\frac{4\pi y(x)}{\lambda}} e^{-i\frac{2\pi mx}{\lambda}} dx \right|^2$$



Dynamic Analysis

Coupled Electrostatic/Structural/Gas Flow Analysis



Continuum Model

Coupled Structural Analysis & Gas Dynamics

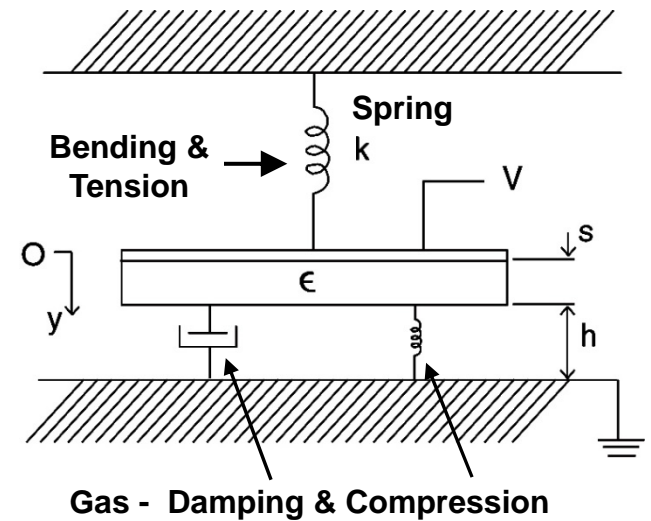
$$\rho A \frac{\partial^2 y}{\partial t^2} - \gamma_{gas} \frac{\partial y}{\partial t} + EI \frac{\partial^4 y}{\partial x^4} - T_{beam} \frac{\partial^2 y}{\partial x^2} = p_{gas}(y) + F_e(y)$$

⊕

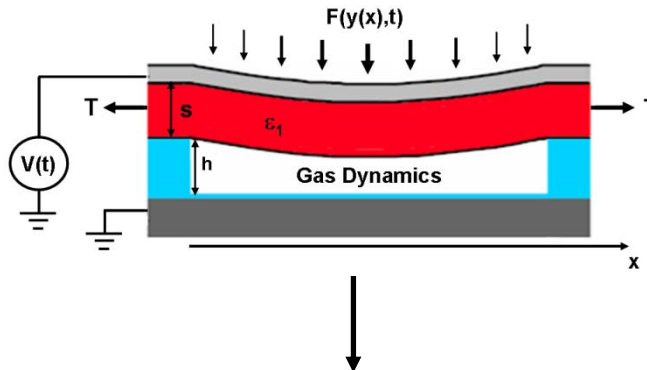
$$\nabla \left(\frac{h^3(x, t)}{12\mu} p_{gas} (\nabla p_{gas}) \right) = \frac{\partial (h(x, t) p_{gas})}{\partial t}$$

Coupling: Gas Flow Influences Microbeam Dynamics

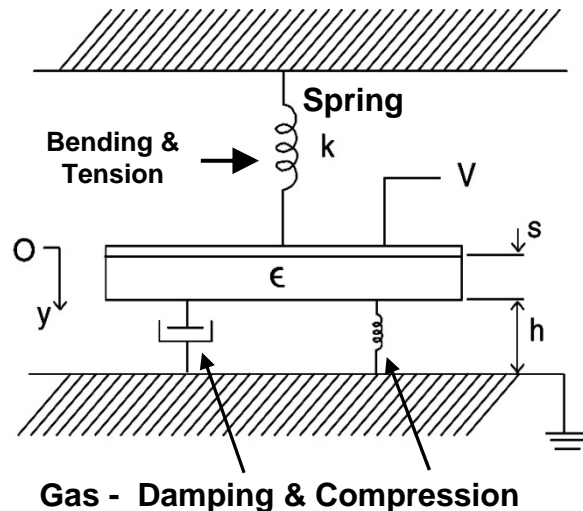
Lumped-Element Model
Damped Spring/Mass System



Continuum to Lumped-Element Model



Lumped-Element Model
Damped Spring/Mass System



Continuum Analysis
 $y(x)$ = displacement along microbeam

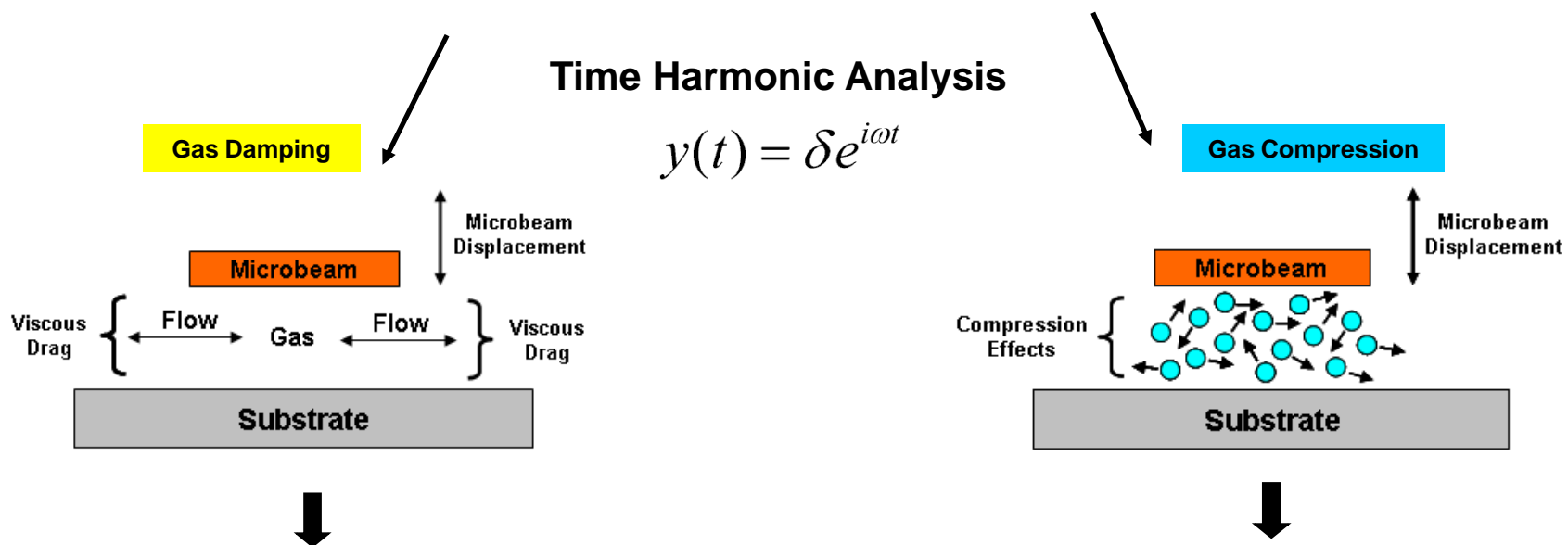
$$\rho A \frac{\partial^2 y}{\partial t^2} - \gamma_{gas} \frac{\partial y}{\partial t} + EI \frac{\partial^4 y}{\partial x^4} - T_{beam} \frac{\partial^2 y}{\partial x^2} = p_{gas}(y) + f_e(y, t)$$

$$m_{eq} \frac{d^2 y}{dt^2} + \underbrace{\gamma_{gas} \frac{dy}{dt}}_{\text{Gas Damping}} + \underbrace{k_{beam} y}_{\text{Bending \& Tension}} + \underbrace{k_{gas} y}_{\text{Gas Compression}} = \underbrace{F_e(y, t)}_{\text{Electrostatic Force}}$$

Lumped-Element Analysis
 y = displacement of midpoint of microbeam

Lumped-Element Dynamic Analysis

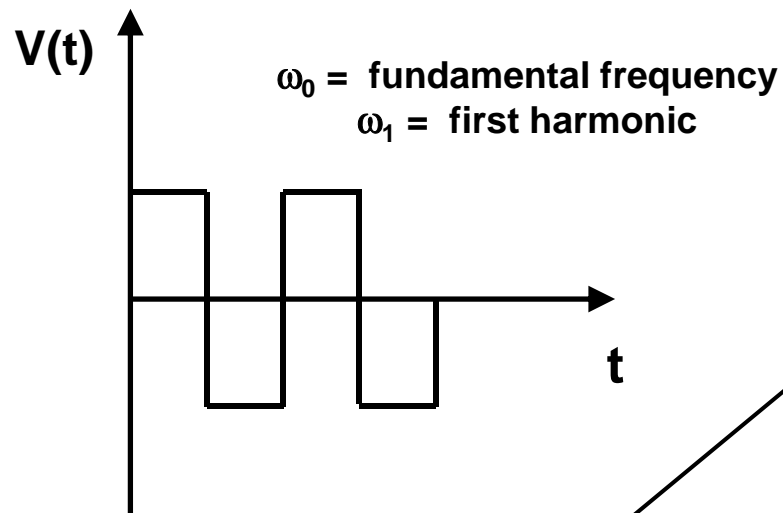
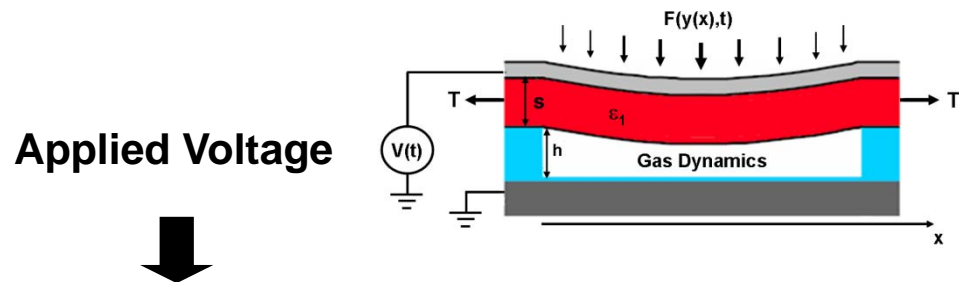
$$m_{eq} \frac{d^2y}{dt^2} + \underbrace{\gamma_{gas} \frac{dy}{dt}}_{\text{Gas Damping}} + \underbrace{k_{beam}y}_{\text{Bending & Tension}} + \underbrace{k_{gas}y}_{\text{Gas Compression}} = \underbrace{F_e(y, t)}_{\text{Electrostatic Force}}$$



$$\gamma_{gas}(\omega) = \frac{64\sigma^2(\omega)P_a A}{\pi^8 h_0} \sum_{m=1,3,\dots}^{\infty} \sum_{n=1,3,\dots}^{\infty} \frac{1}{(mn)^2 \left[(m^2 + \beta^2 n^2)^2 + \sigma^2(\omega) / \pi^4 \right]}$$

$$k_{gas}(\omega) = \frac{64\sigma(\omega)P_a A}{\pi^6 h_0} \sum_{m=1,3,\dots}^{\infty} \sum_{n=1,3,\dots}^{\infty} \frac{m^2 + \beta^2 n^2}{(mn)^2 \left[(m^2 + \beta^2 n^2)^2 + \sigma^2(\omega) / \pi^4 \right]}$$

Effective Modeling Parameters



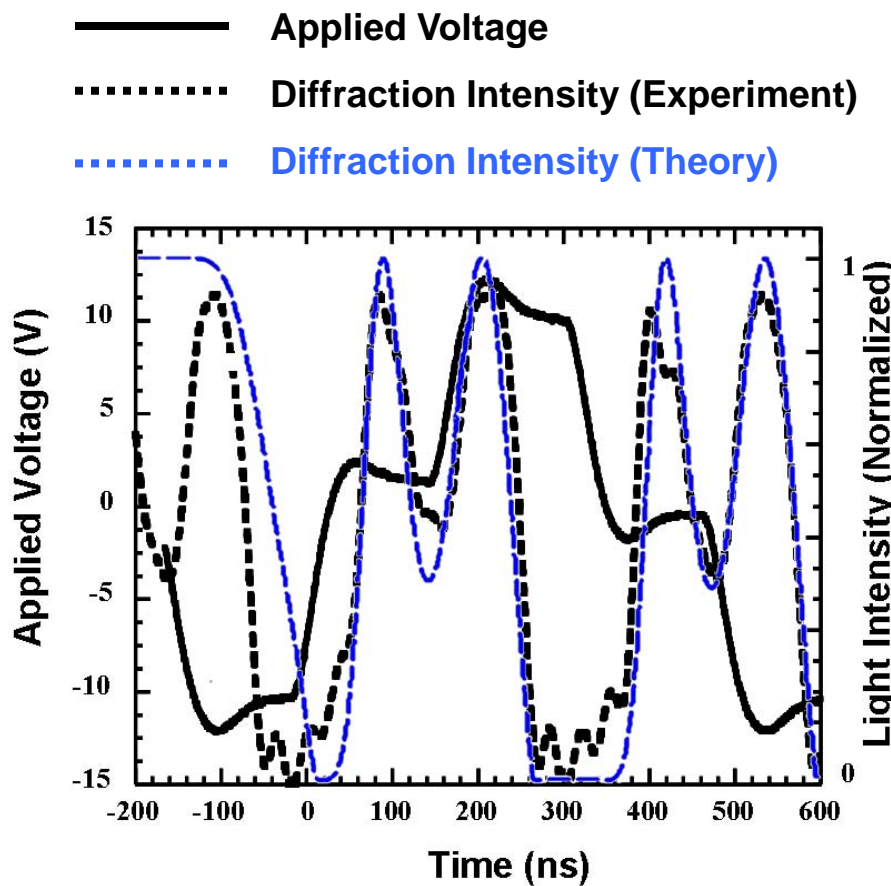
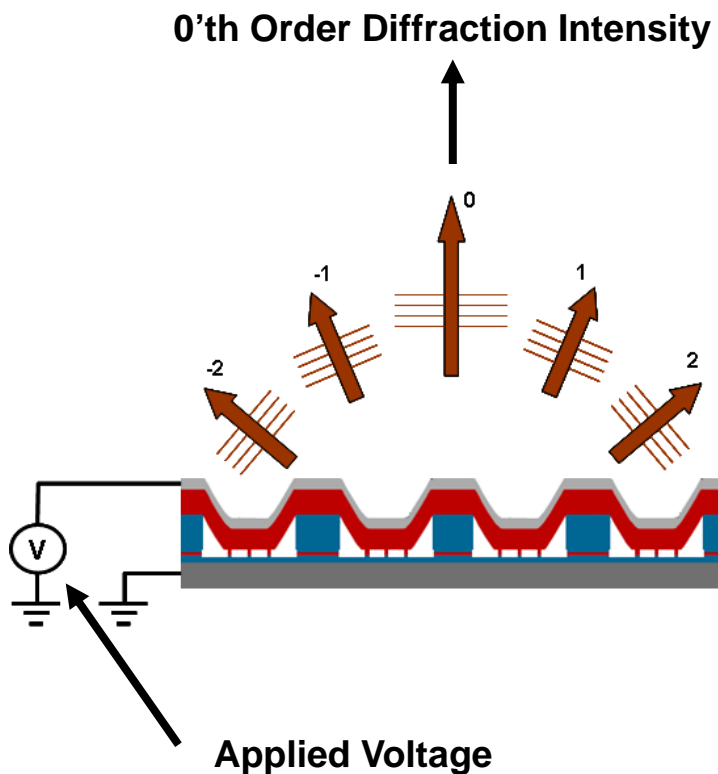
$$\hat{\gamma}_{gas} = \frac{\gamma_{gas}(\omega_0) + \gamma_{gas}(\omega_1)}{2}$$

$$\hat{k}_{gas} = \frac{k_{gas}(\omega_0) + k_{gas}(\omega_1)}{2}$$

$$m_{eq} \frac{d^2y}{dt^2} + \underbrace{\hat{\gamma}_{gas} \frac{dy}{dt}}_{\text{Gas Damping}} + \underbrace{\frac{k_{beam}y}{\varepsilon_0 s}}_{\text{Bending & Tension}} + \underbrace{\frac{\hat{k}_{gas}y}{\varepsilon_0 s}}_{\text{Gas Compression}} = \frac{\varepsilon^2 \varepsilon_0 A}{2} \frac{V^2(t)}{[\varepsilon_0 s + \varepsilon(h - y)]^2}$$

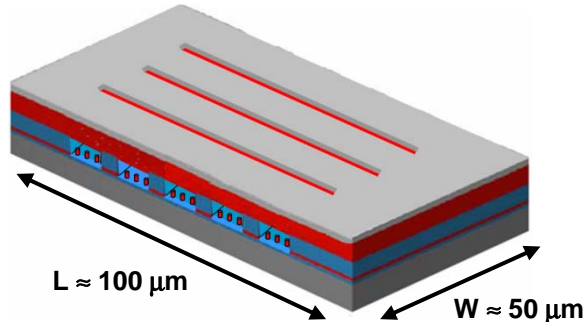
Lumped-Element Model vs. Experiment

Prediction of Diffraction Intensity into 0'th Order vs. Applied Voltage

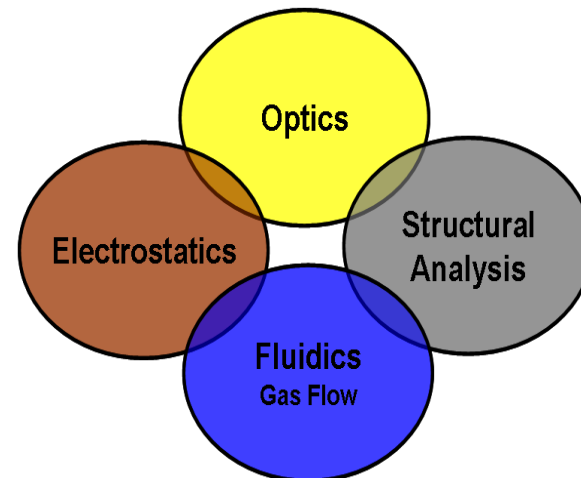
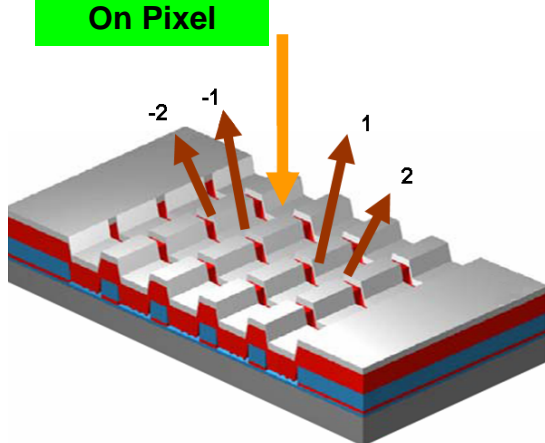


Summary

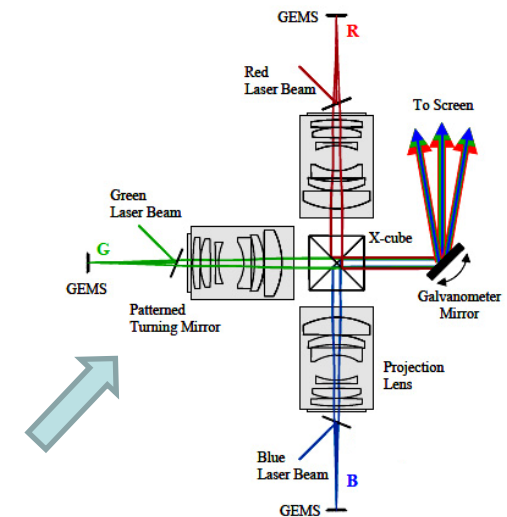
Off Pixel



On Pixel

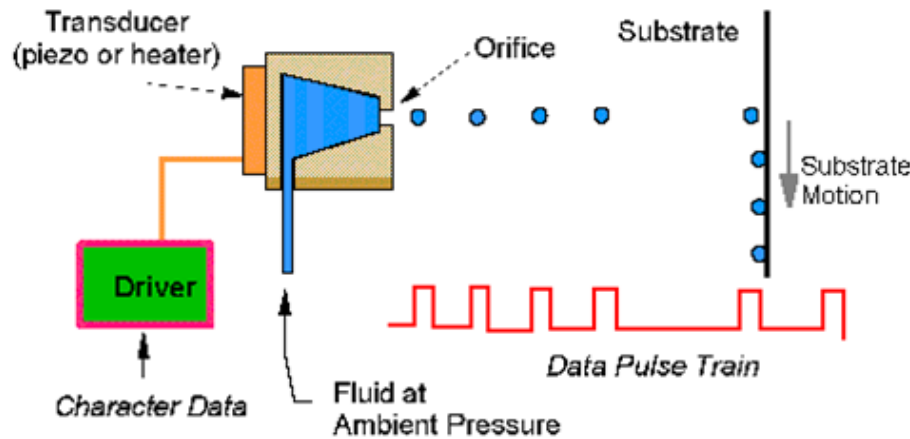


- Operating Voltage
- Microbeam Deformation Profile
- Diffraction Efficiency
- Dynamic Response of Microbeam



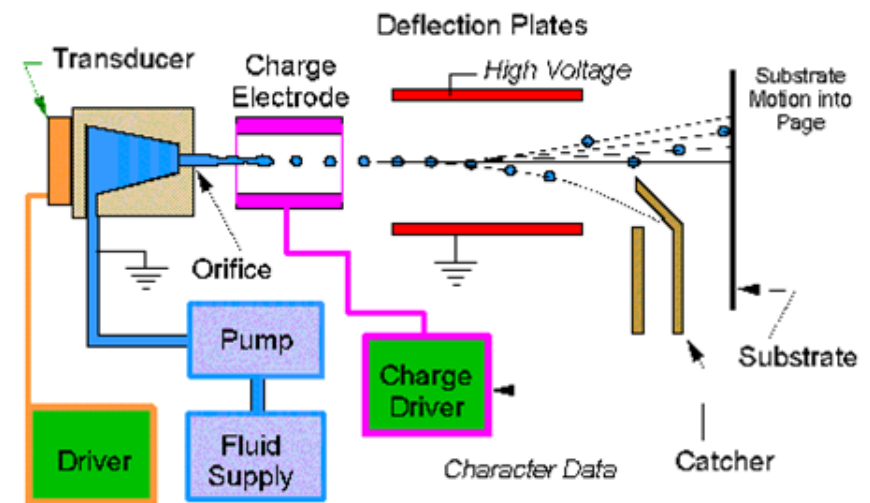
Microfluidics: Inkjet Printing

Drop-on-Demand (DOD) Printing



30,000 Drops Generated per sec from each Nozzle

Continuous Printing



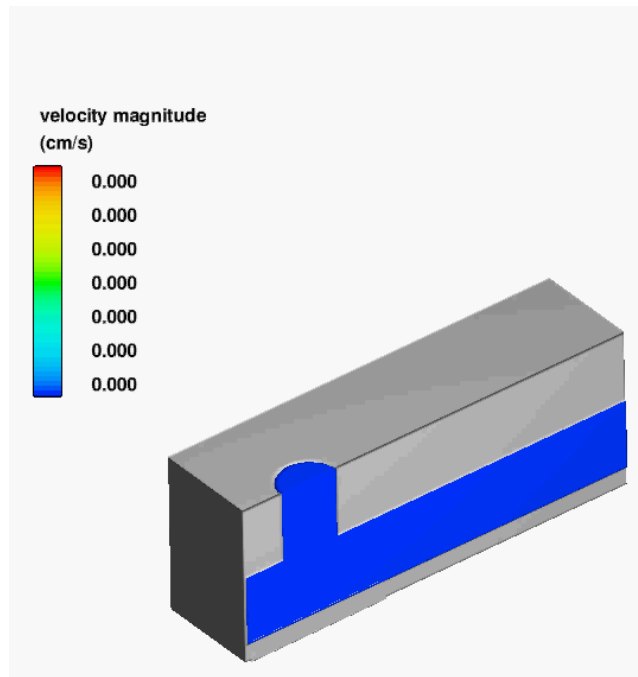
500,000 Drops Generated per sec from each Nozzle

Motivation

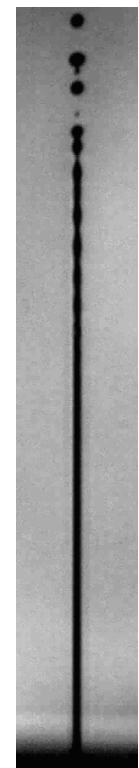
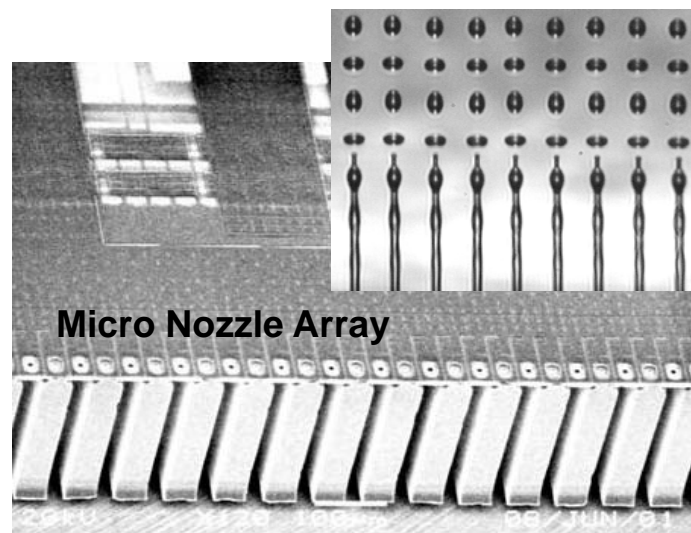
Microfluidic-based Printing: Most Successful Microfluidic Application (\$50-100B)

Microfluidics: Inkjet Technology

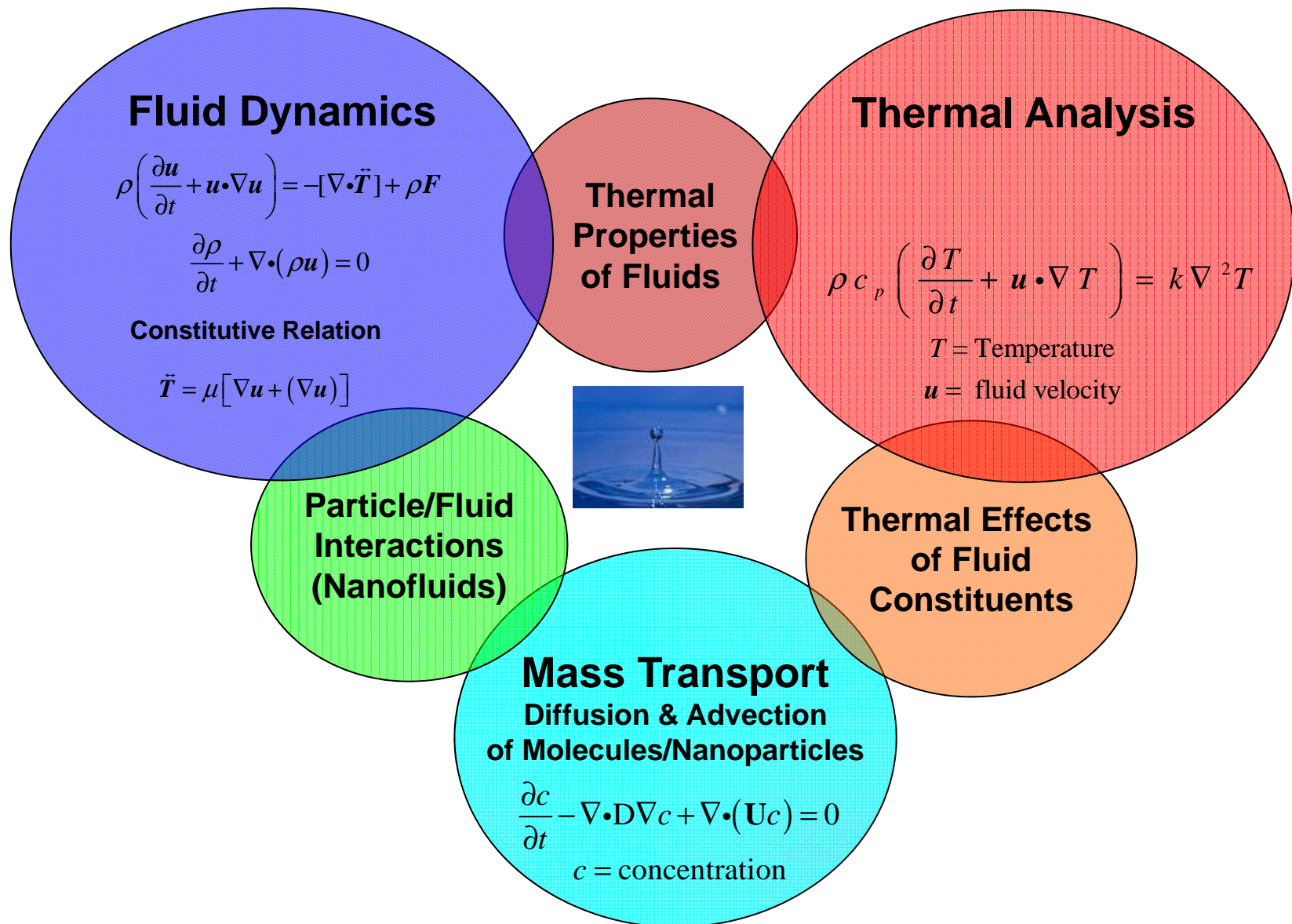
Drop-on-Demand (DOD) Printing



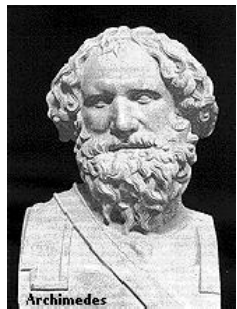
Continuous Printing



Fluid Dynamics and Transport Phenomena



Historical Contributions to Fluid Mechanics



Archimedes
(C. 287-212 BC)



Newton
(1642-1727)



Leibniz
(1646-1716)



Bernoulli
(1667-1748)



Euler
(1707-1783)



Navier
(1785-1836)
57:020 Fluid Mechanics



Stokes
(1819-1903)



Reynolds
(1842-1912)



Prandtl
(1875-1953)



Taylor
(1886-1975)

Hydrodynamics

Governing Equations based on the Laws of Physics

- **Conservation of Mass** (ρ = fluid density, u = fluid velocity).

$$\frac{\partial \rho}{\partial t} + \nabla \cdot (\rho u) = 0$$

- **Newton's Second Law**: the change of momentum equals the sum of forces (p = pressure, μ = viscosity, f = external force density).

$$\rho \left(\frac{\partial u}{\partial t} + u \cdot \nabla u \right) = -\nabla p + \mu \nabla^2 u + f$$

- **Conservation of Energy - First Law of Thermodynamics**
(T = fluid temperature)

$$\rho c_p \left(\frac{\partial T}{\partial t} + u \cdot \nabla T \right) = k \nabla^2 T$$

Navier-Stokes Equations



Newton's Second Law: change of momentum equals the sum of forces (p = pressure, μ = viscosity, f = external force density).

Claude Navier
1785-1836

Georges Stokes
1819-1903

3D Cartesian Coordinates

$$\rho \frac{\partial u}{\partial t} + \rho u \frac{\partial u}{\partial x} + \rho v \frac{\partial u}{\partial y} + \rho w \frac{\partial u}{\partial z} = - \frac{\partial p}{\partial x} + \mu \left[\frac{\partial^2 u}{\partial x^2} + \frac{\partial^2 u}{\partial y^2} + \frac{\partial^2 u}{\partial z^2} \right]$$

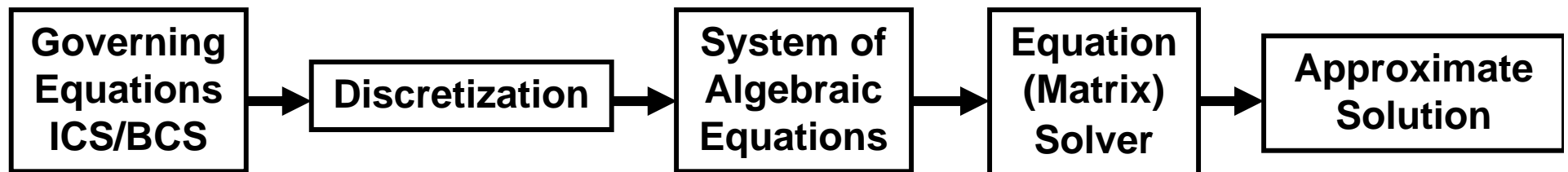
$$\rho \frac{\partial v}{\partial t} + \rho u \frac{\partial v}{\partial x} + \rho v \frac{\partial v}{\partial y} + \rho w \frac{\partial v}{\partial z} = - \frac{\partial p}{\partial y} + \mu \left[\frac{\partial^2 v}{\partial x^2} + \frac{\partial^2 v}{\partial y^2} + \frac{\partial^2 v}{\partial z^2} \right]$$

$$\rho \frac{\partial w}{\partial t} + \rho u \frac{\partial w}{\partial x} + \rho v \frac{\partial w}{\partial y} + \rho w \frac{\partial w}{\partial z} = - \frac{\partial p}{\partial z} + \mu \left[\frac{\partial^2 w}{\partial x^2} + \frac{\partial^2 w}{\partial y^2} + \frac{\partial^2 w}{\partial z^2} \right]$$



The Navier Stokes equations are very difficult to solve analytically because they are non-linear. Analytical solutions exist for few albeit very important cases such laminar flow through regularly shaped conduits!

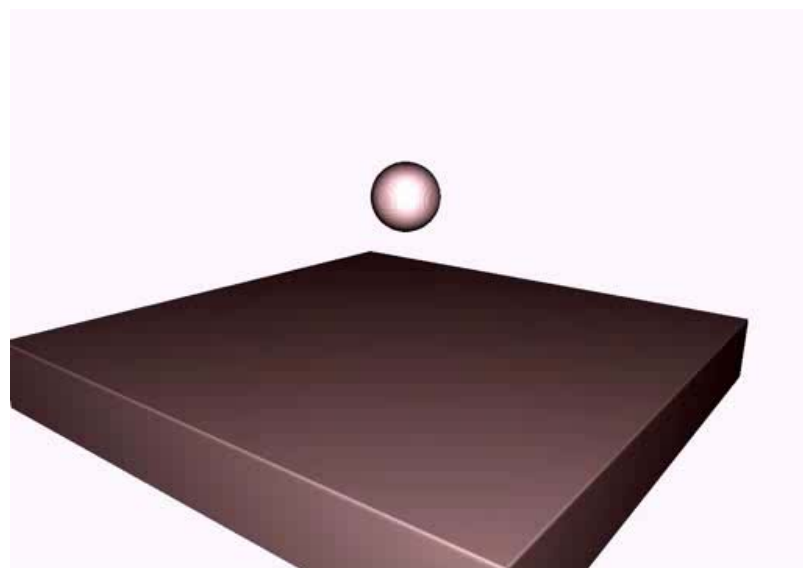
Numerical Approach to Solving PDEs



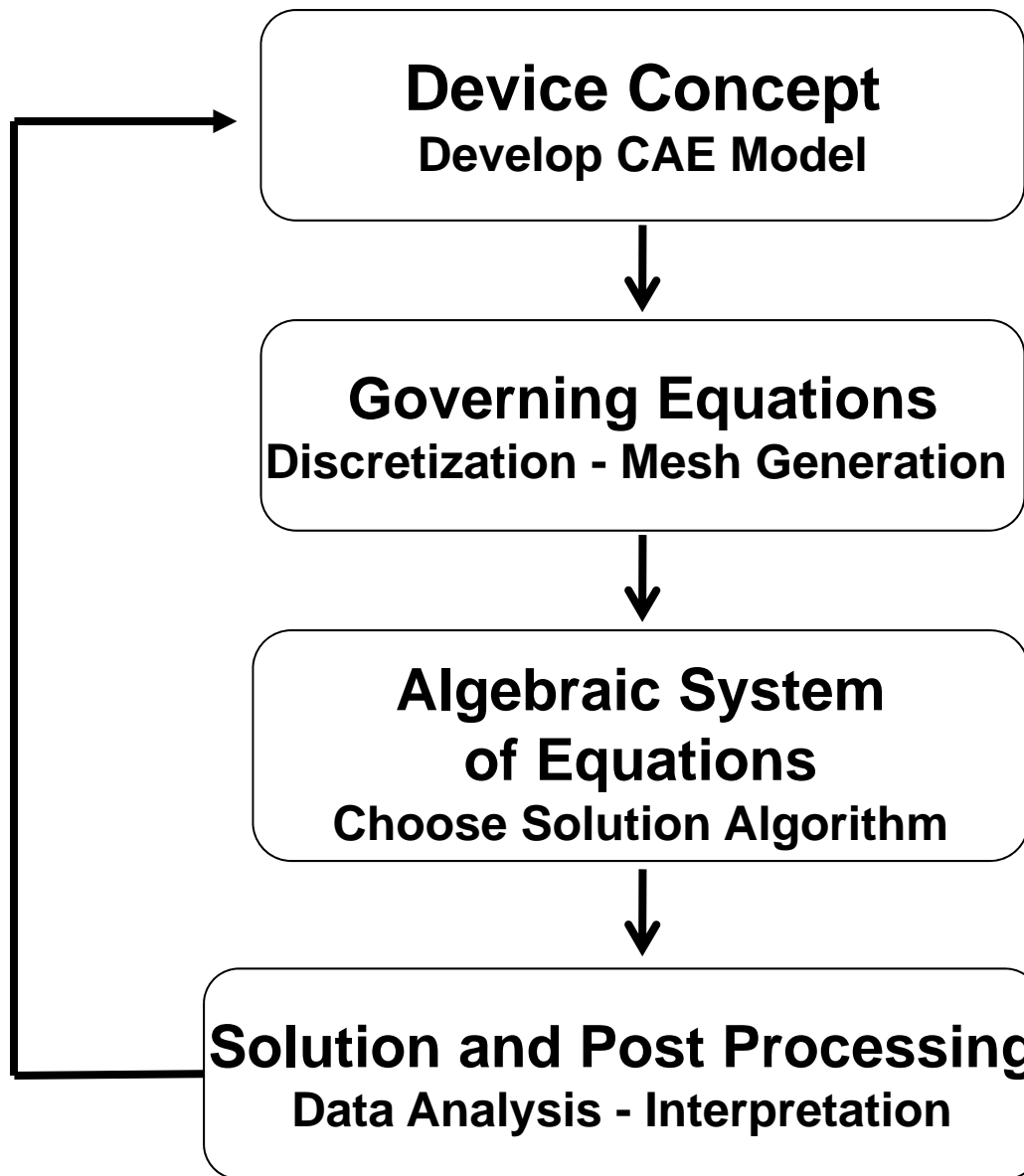
Continuous Solutions	Finite-Difference Finite-Volume Finite-Element Spectral Methods Boundary Element	Discrete Nodal Values	Tridiagonal ADI SOR Gauss-Seidel Conjugate gradient Gaussian elimination	$u_i(x,y,z,t)$ $p(x,y,z,t)$ $T(x,y,z,t)$
----------------------	--	-----------------------	---	--

What is Computational Fluid Dynamics (CFD)?

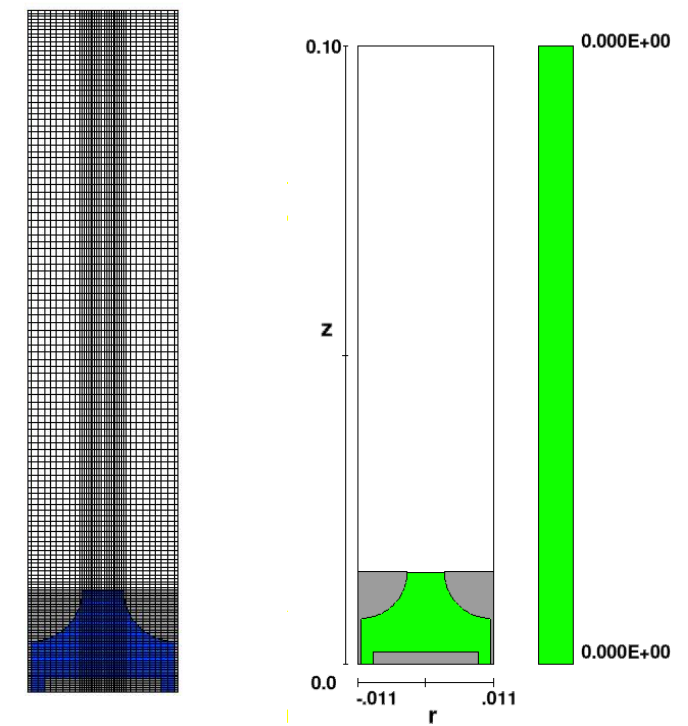
Computational fluid dynamics (CFD) is the science of predicting the behavior of fluid flow and related transport phenomena, e.g. heat transfer, chemical kinetics etc., by solving the governing equations using numerical methods.



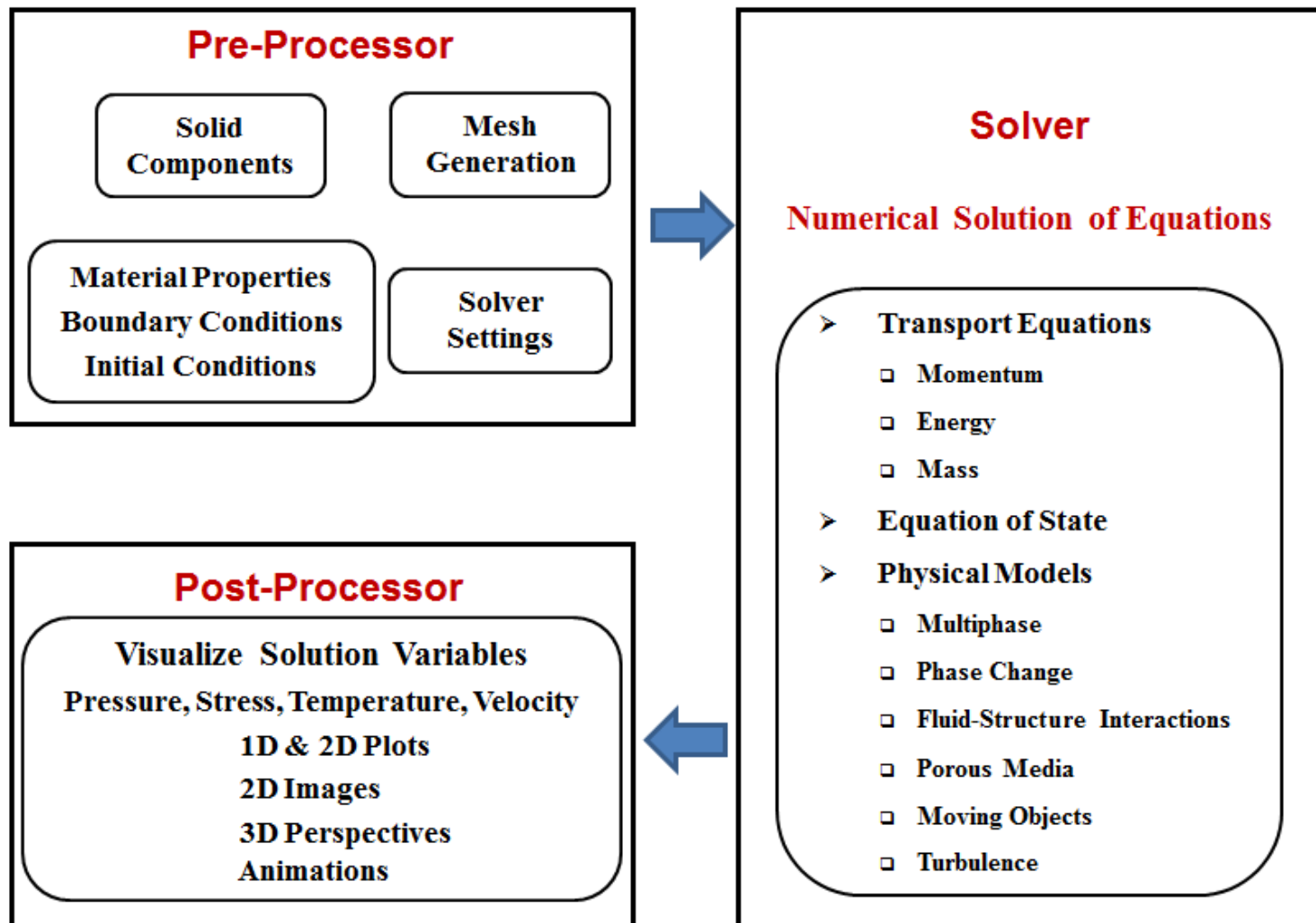
CFD Modeling Cycle



Piston Driven
Droplet Generation



CFD Program Solution Cycle

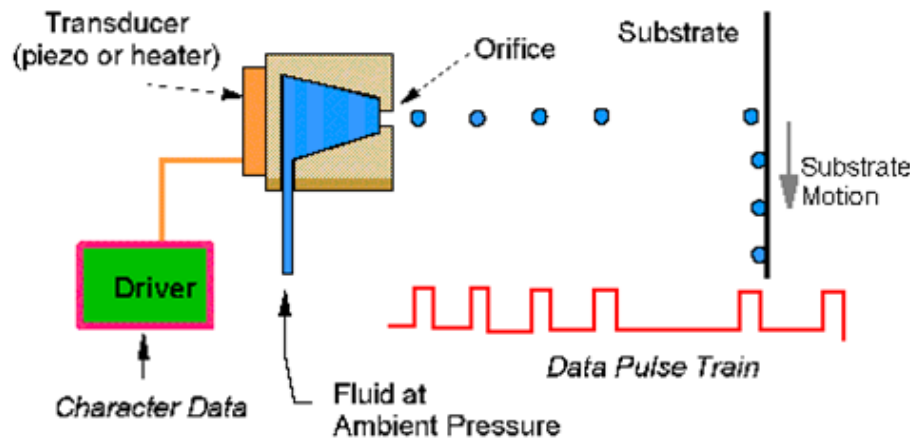


CFD Analysis Applied to Inkjet Printing

- **Inkjet Printing Methods (DOD & CIJ)**
- **Phase Change Simulation**
- **Thermal-Fluidic & Free-Surface Analysis**
 - Droplet Generation
 - Marangoni-Assisted Jet Instability
- **Particle-Fluid Interactions**
 - Aerodynamic Analysis
 - Nanofluids
- **Fluid-Surface Interactions**

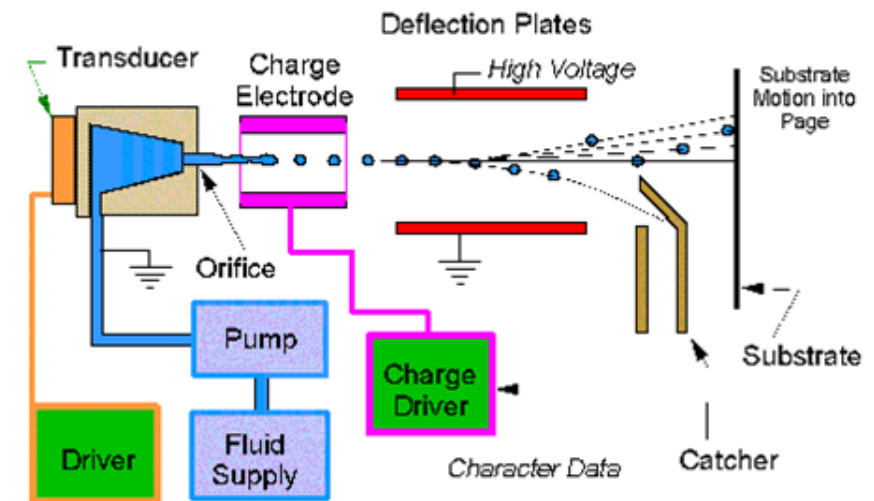
Microfluidic-based Printing

Drop-on-Demand (DOD) Printing



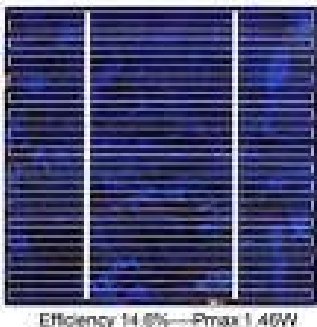
30,000 Drops Generated per sec from each Nozzle

Continuous Printing

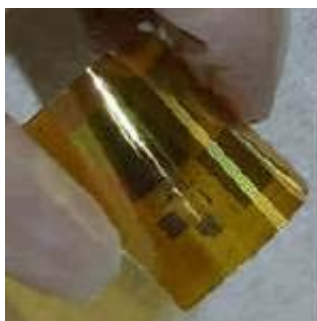


500,000 Drops Generated per sec from each Nozzle

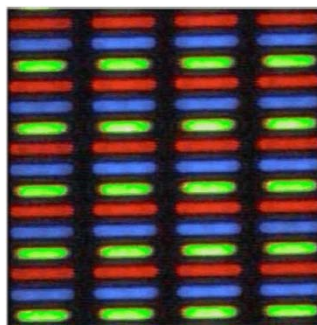
Emerging Microfluidic Printing Applications



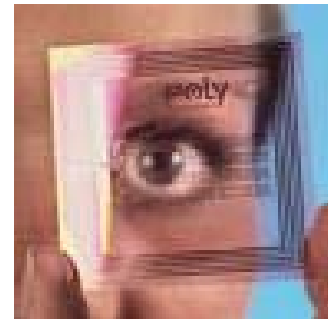
- Photovoltaics
- Fuel Cells
- Batteries



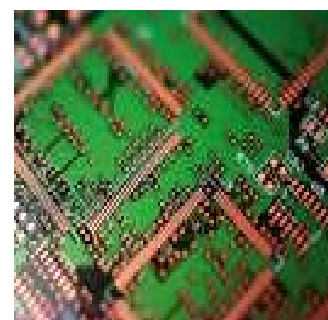
- Flex circuits
- Smart Textiles
- PCB Photomasks
- Interconnects



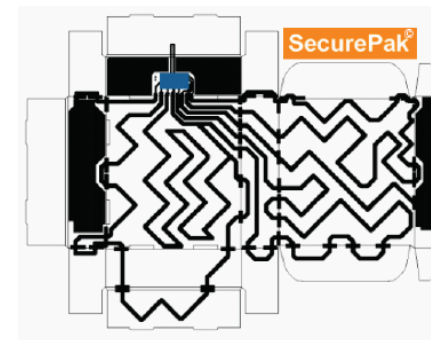
- Flat Panel Display
- PLED
- LCD
- Color filters
- Flexible displays



- RF- ID
- Antennas



- Printed Circuit Boards

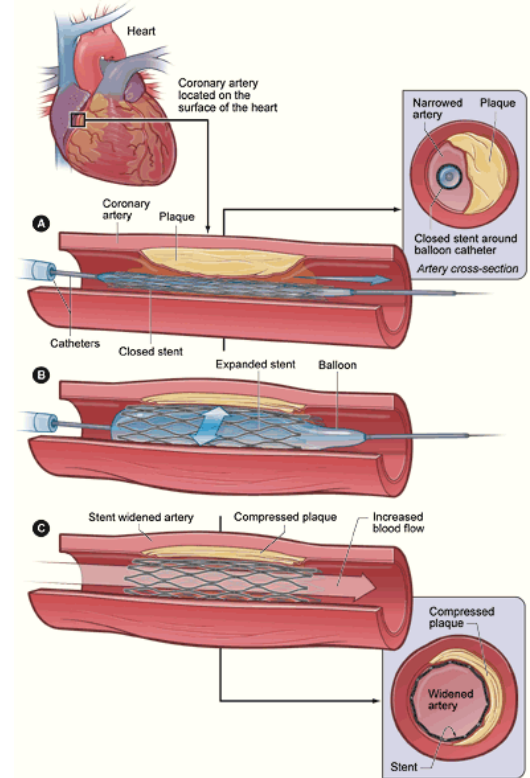


- Smart Packaging

Coating of Stents

Stent - fabricated from metals/alloys/polymers and surface treated with materials that reduce the rejection mechanisms.

Current coating methods: dipping, ultrasonic spray coating, painting (air brush), and deposition along the struts using syringes.

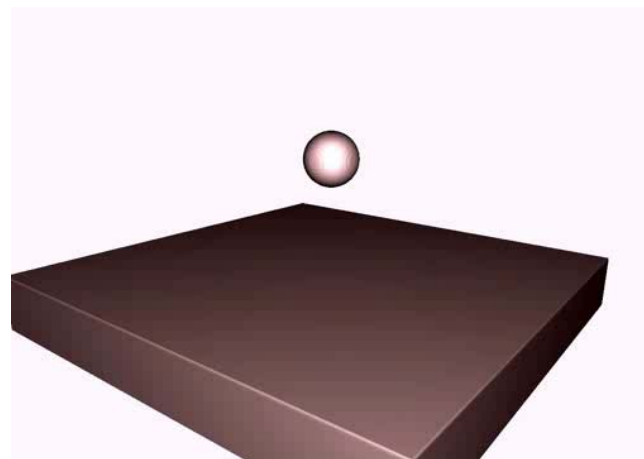


Ink-jet based Stent coating

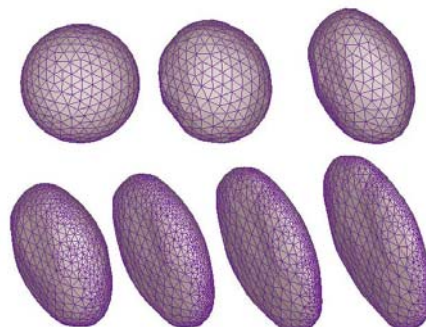


Multiphase Computational Fluid Dynamics (CFD)

Tracking an Interface

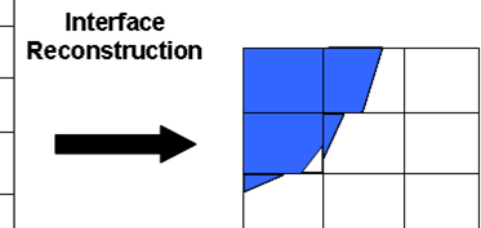


Lagrangian Methods
(Adaptive Grid)



Eulerian Methods
(Fixed Grid)

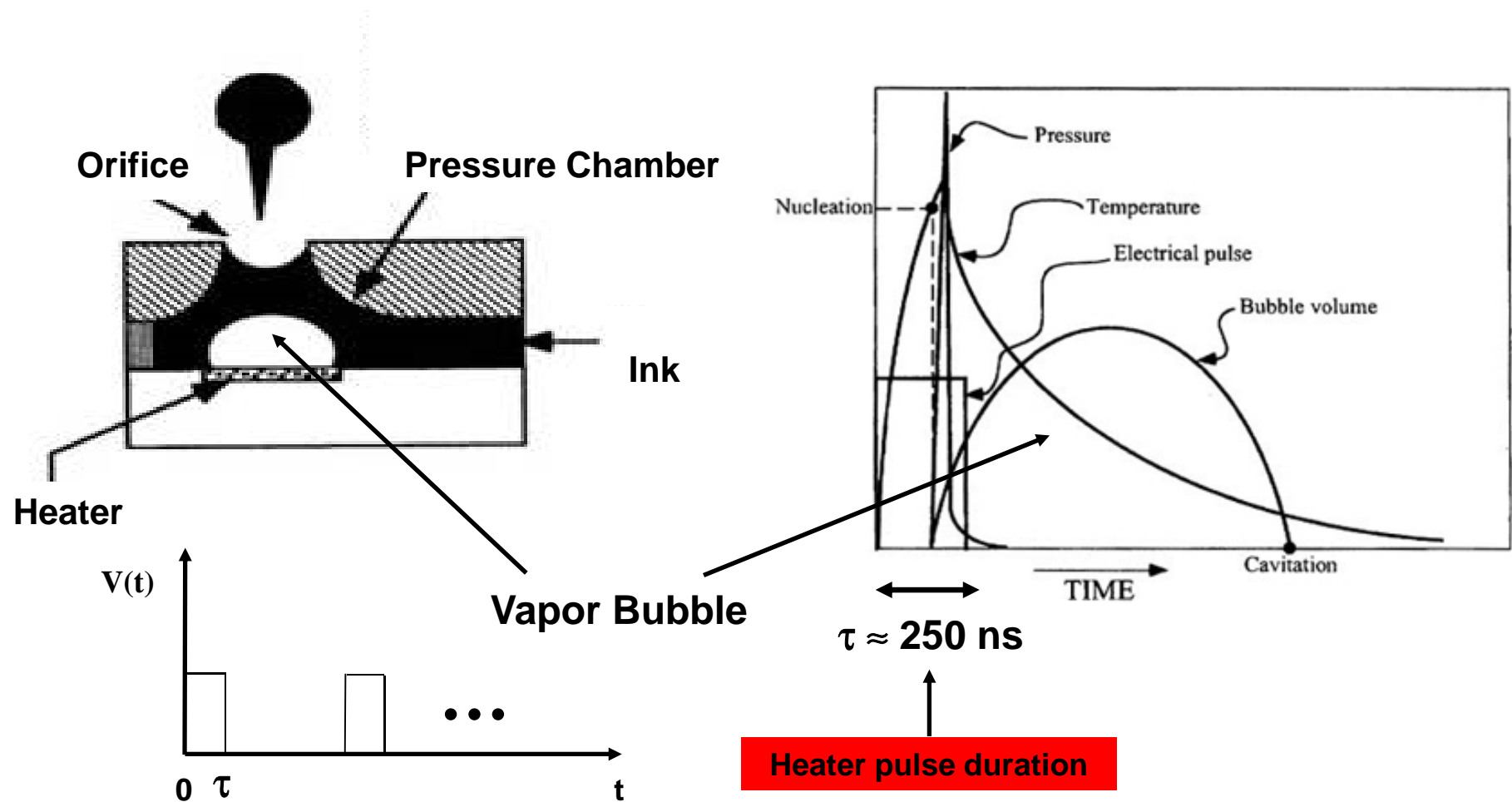
1	1	1	.68	0
1	1	1	.42	0
1	1	.92	.09	0
1	.85	.35	0	0
.31	.09	0	0	0
0	0	0	0	0



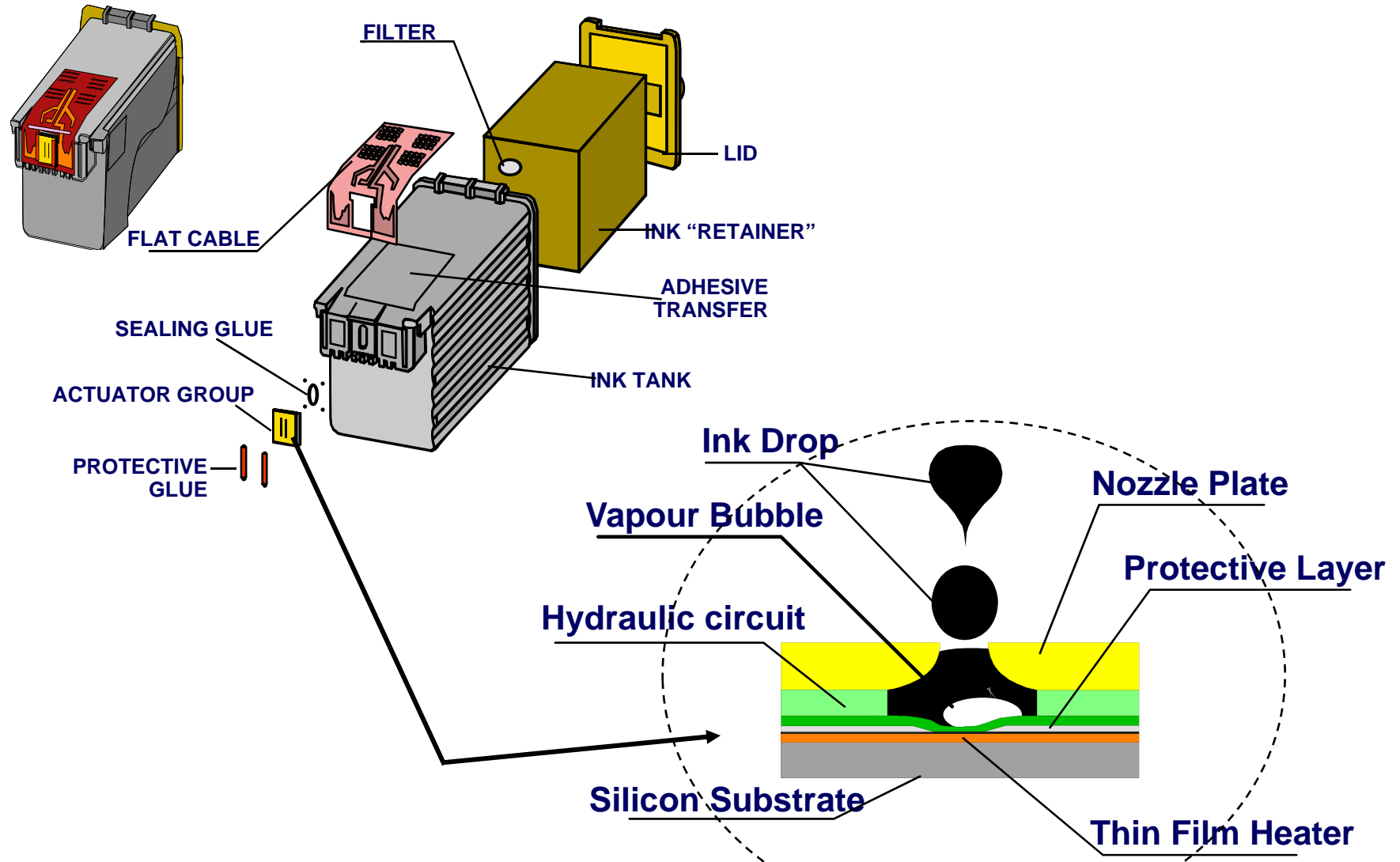
Volume of Fluid (VOF) Method*

Drop-on-Demand Printing

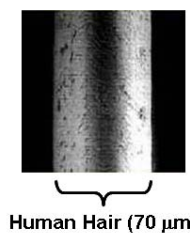
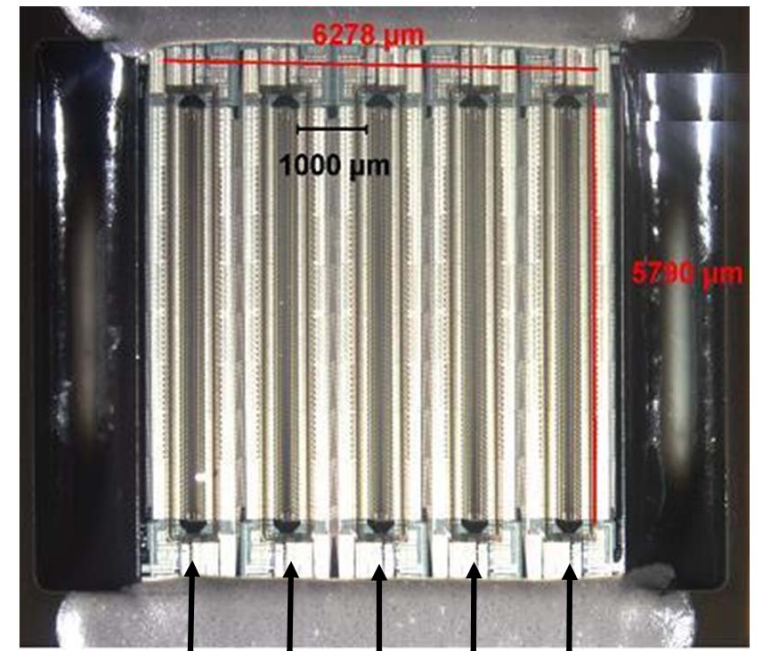
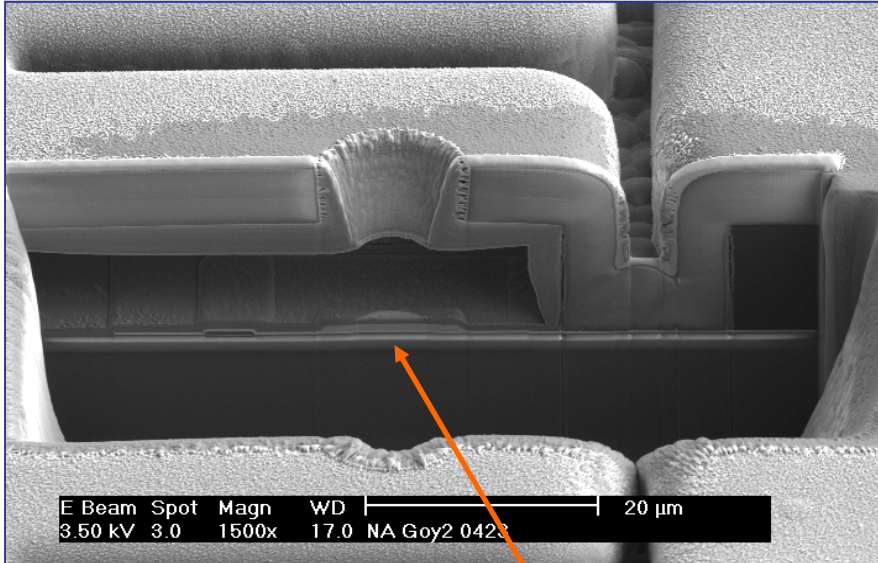
Thermal Bubble Jet



Printing Cartridge - Thermal Bubble Jet

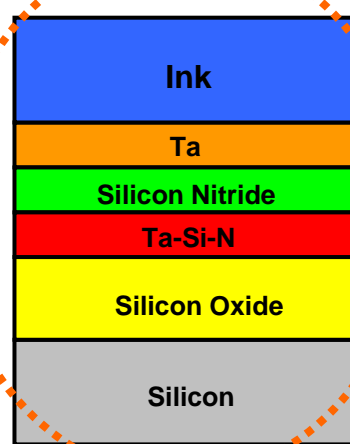
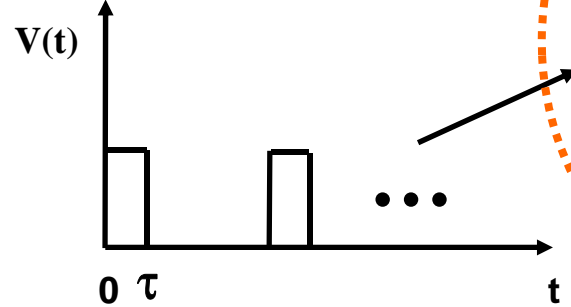


Kodak MEMS Thermal Bubble Jet Drop Ejector



Human Hair (70 μm)

Voltage Applied to
Ta-Si-N Heater Layer



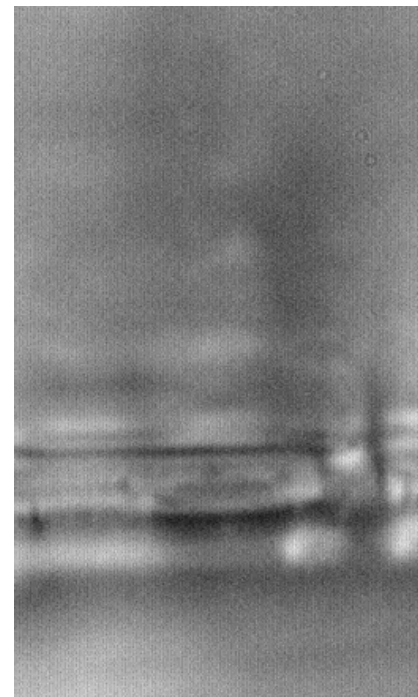
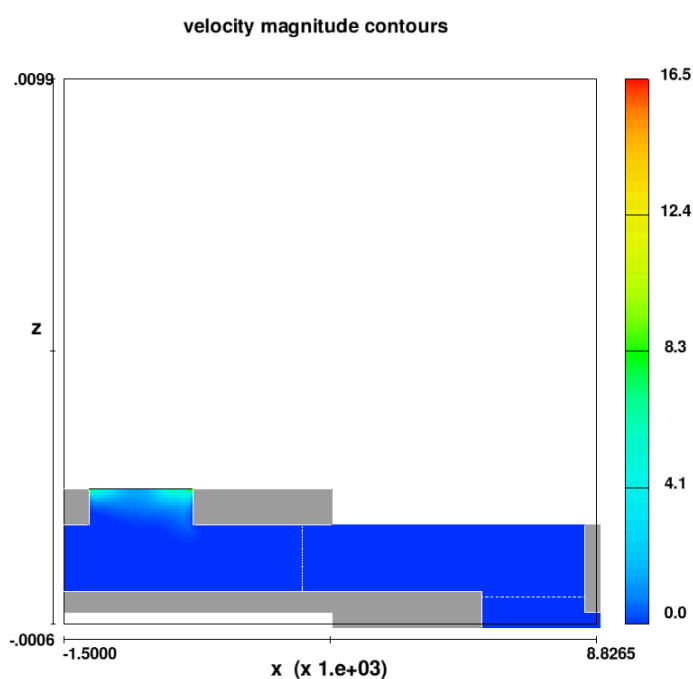
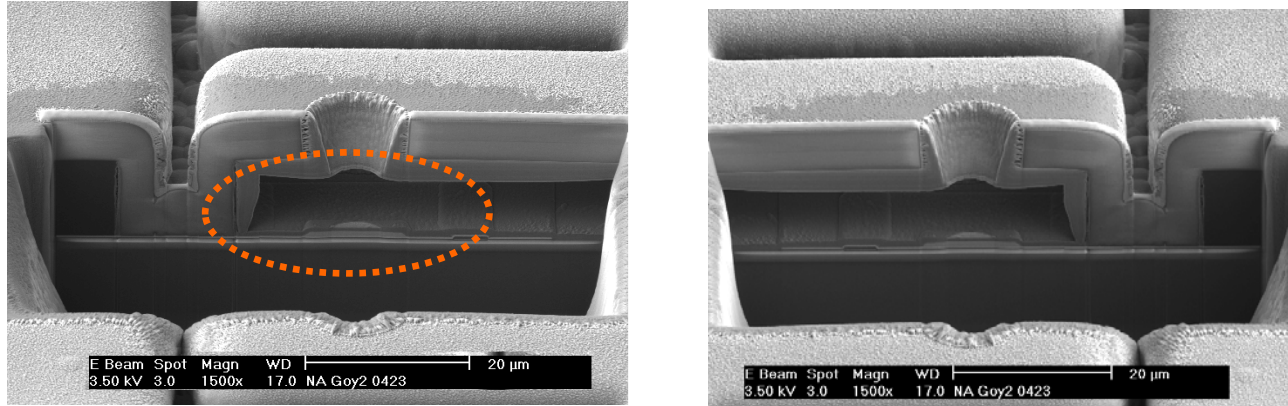
Five ink channels each of which feeds
two arrays of nozzles

Each channel/nozzle array prints a separate color

Ta-Si-N Heater Layer < 0.1 μm

Heater pulse duration: $\tau \approx 250 \text{ ns}$

Thermal Bubble Jet Drop Ejection: Model vs. Experiment



**3D CFD
Phase Change Analysis**

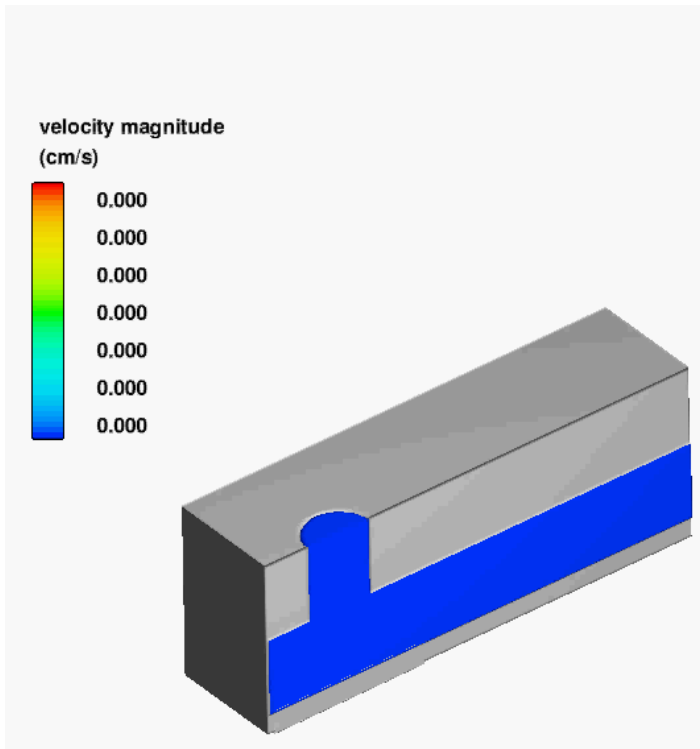
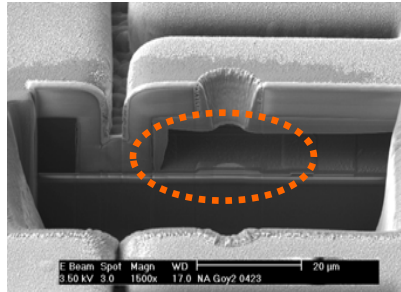
**Homogeneous
Bubble Nucleation
&
Free-Surface Tracking**

**Quad-Core Workstation
2.8 GHz Processors
Windows XP 32 Bit**

Simulation Time = 24 Hrs

Flow 3D - VOF Solver

CFD Thermal Bubble Jet Simulation

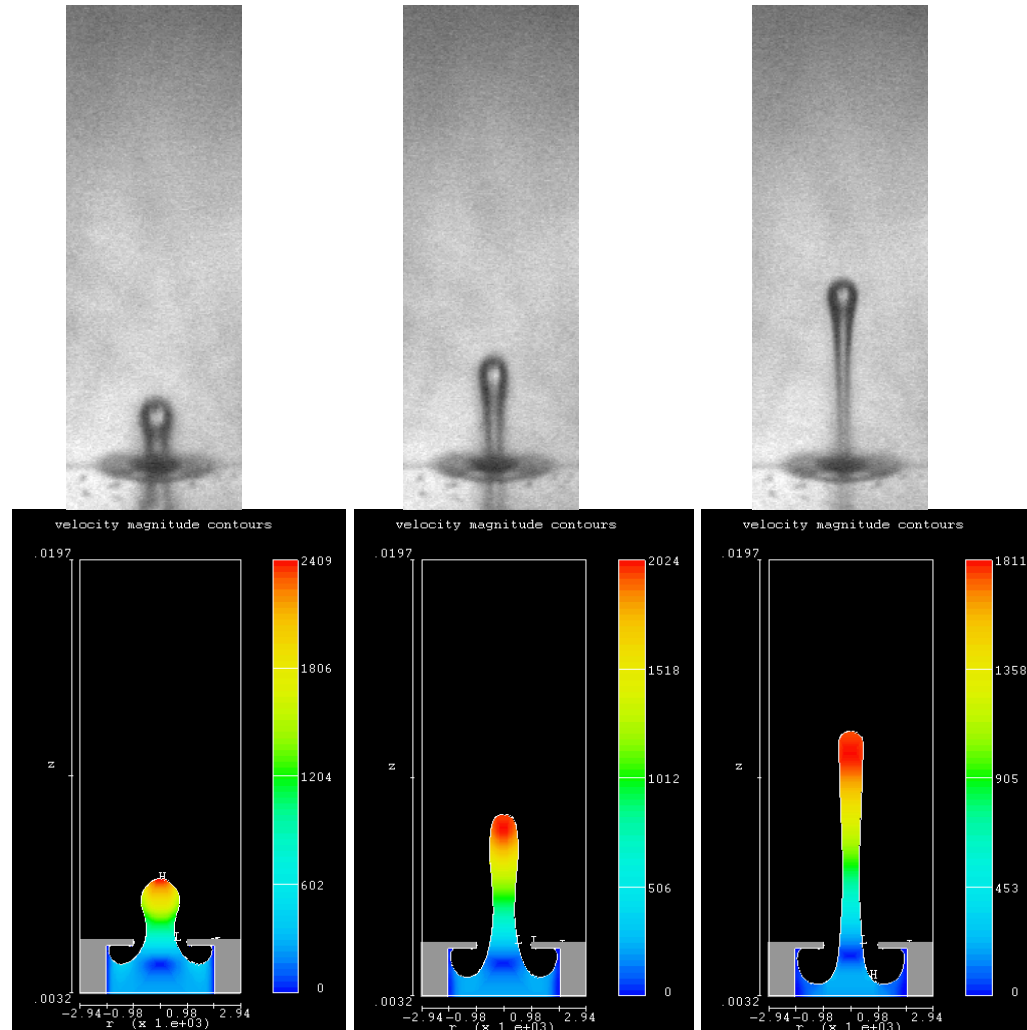


Predicted Volume 6.8pl

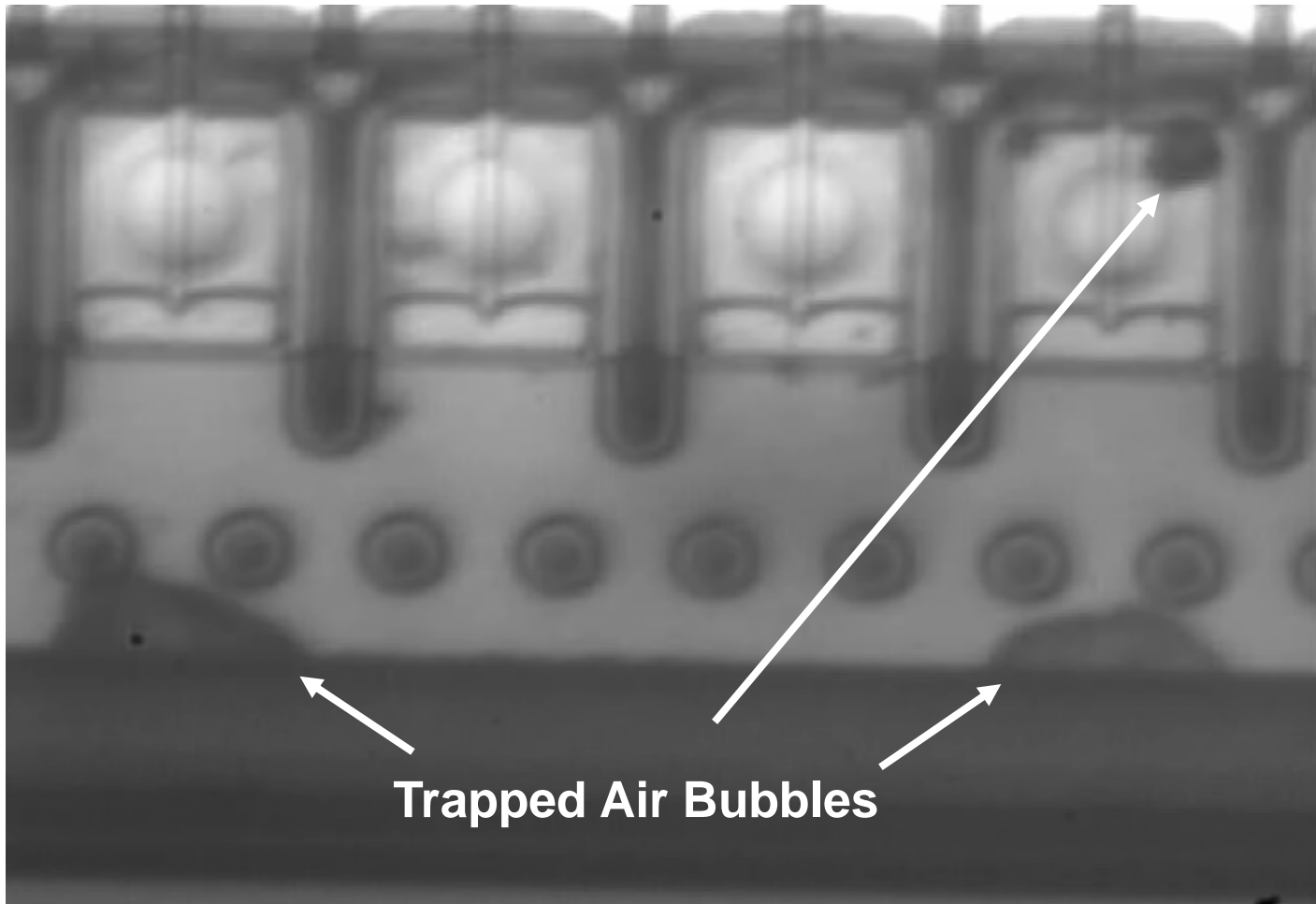
Predicted Velocity 16.5m/s

- 1) Power is applied to a thin film resistive heater.
- 2) Fluid adjacent to the heated structure reaches its superheat limit and a vapor bubble form.
- 3) The bubble expands rapidly, driving fluid through the orifice causing a droplet to be expelled.
- 4) As the vapor bubble expands, a thin layer of superheated fluid which feeds the vapor bubble is depleted, causing the bubble growth to slow, and eventually collapse.

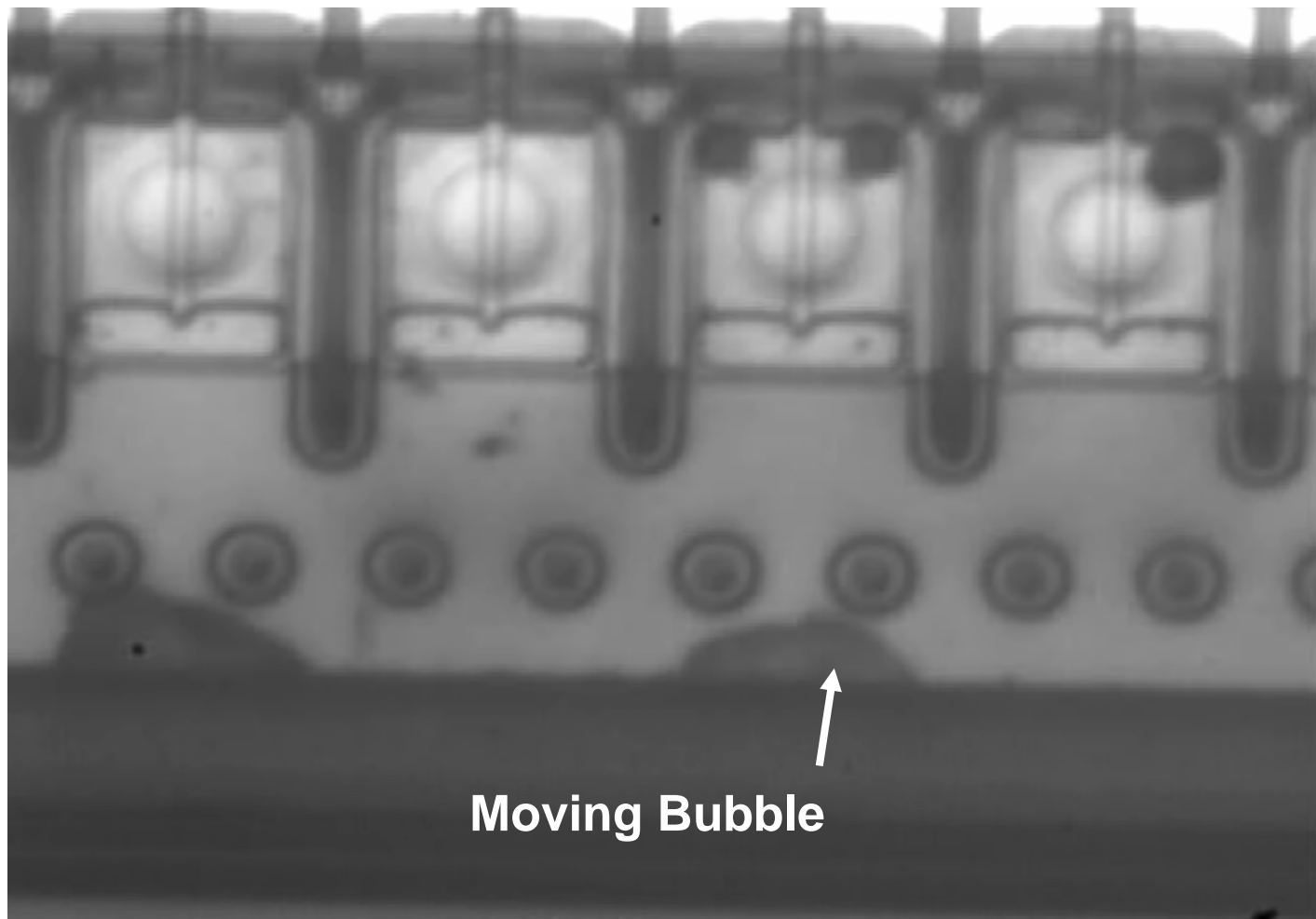
DOD Simulation vs. Experiment



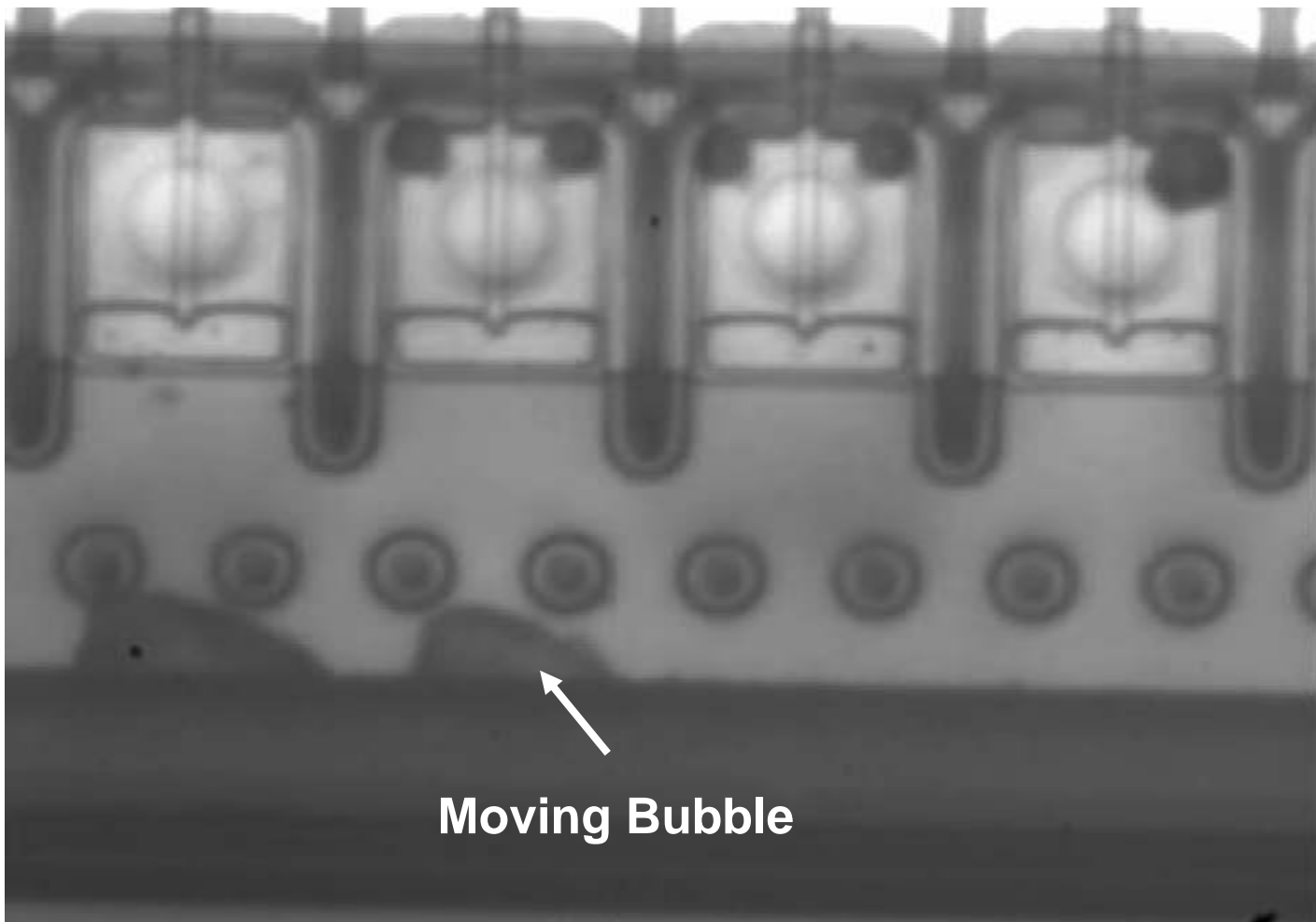
Understanding Air Entrapment - Moving Bubbles



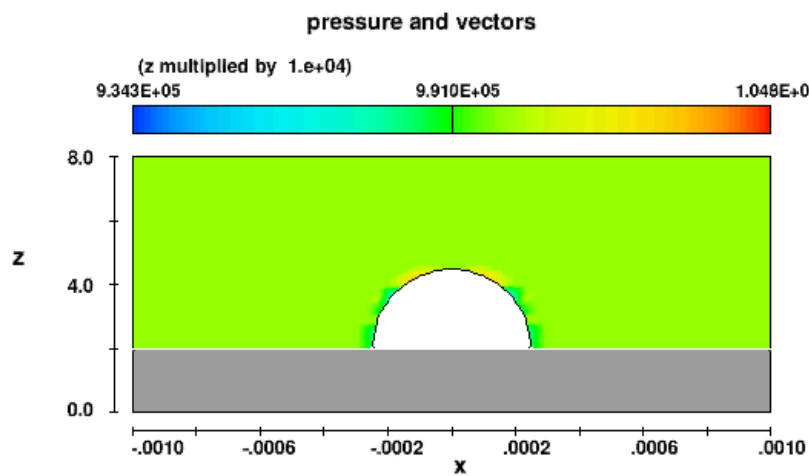
Moving Bubbles



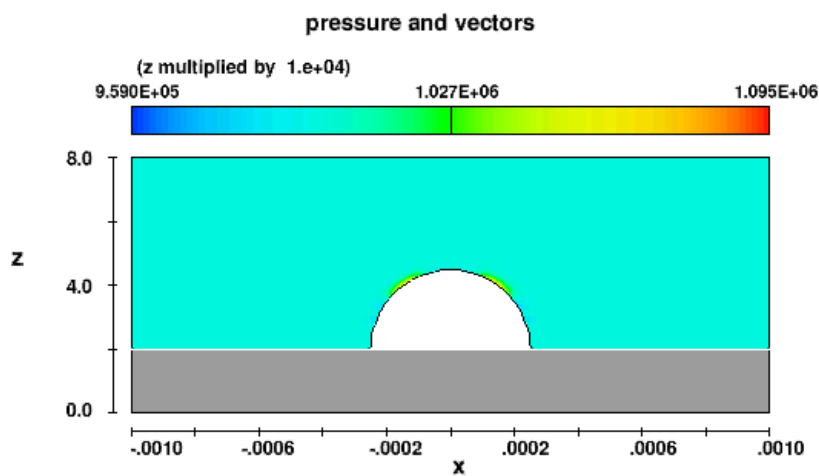
Moving Bubbles



Bubble Movement (3D CFD)



Contact Angle = 90 deg



Contact Angle = 135 deg

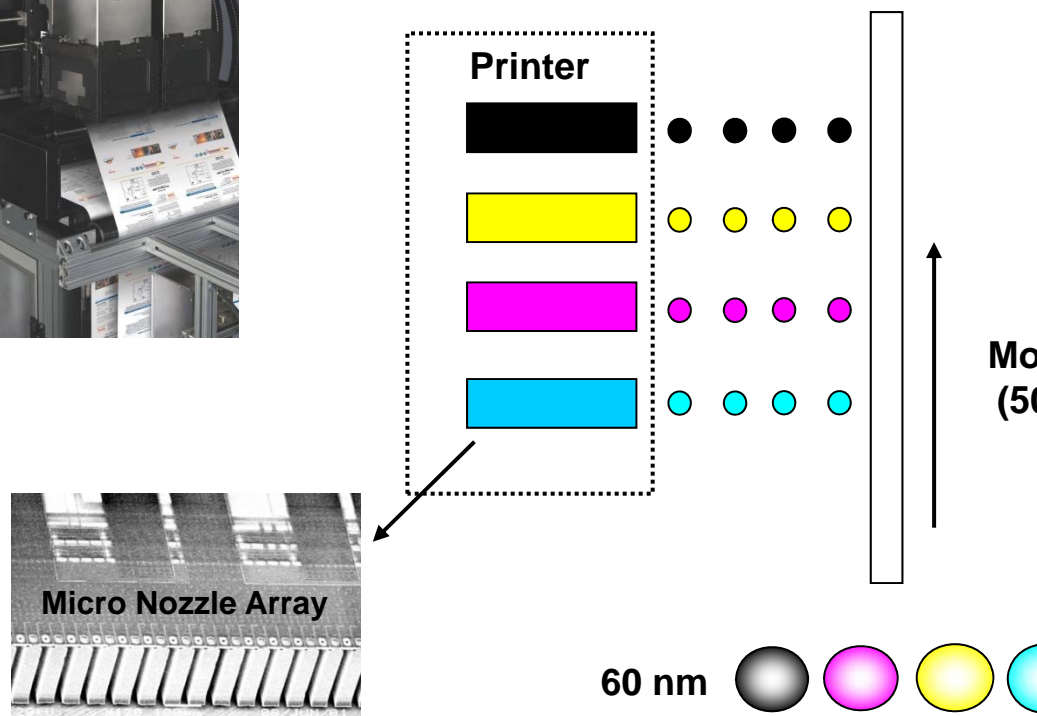
Kodak Stream Technology

Commercial Printer



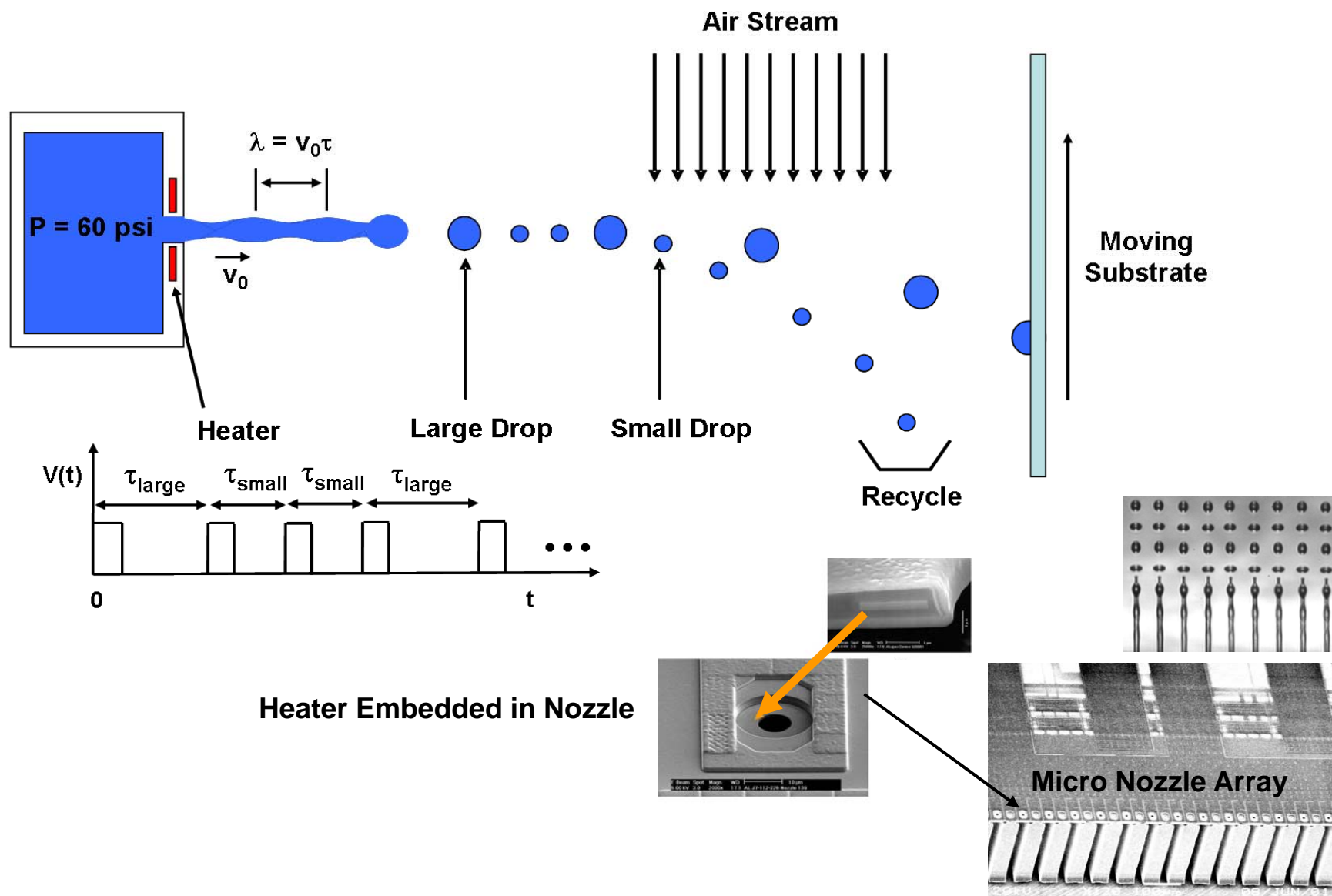
Prints 8x11in Full Color Image in 1 ms
2400 Times Faster Than Home Printer*

Image Quality

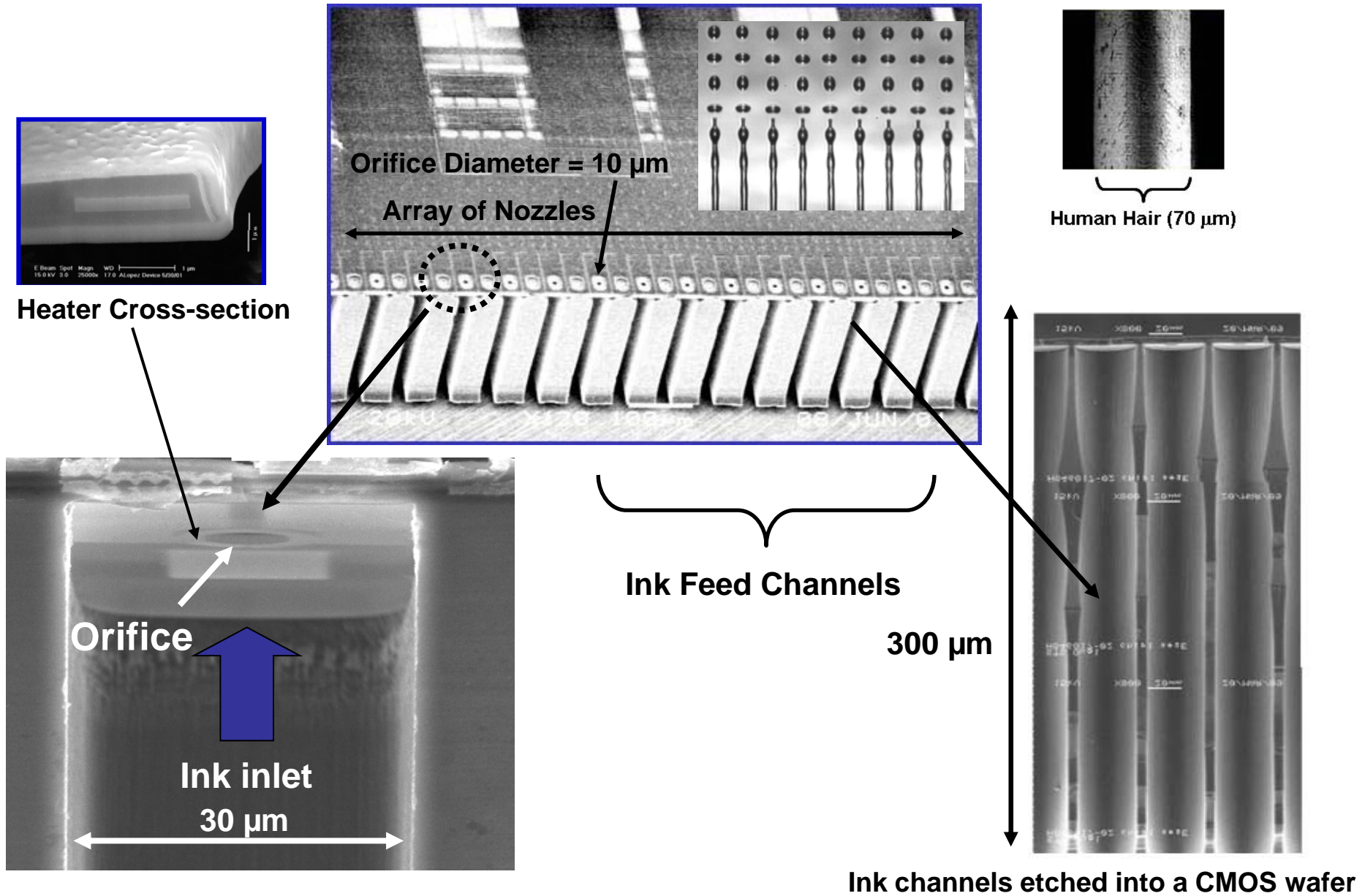


*Assumes 25 color pages printed per minute

Thermally Induced Microdrop Generation



Kodak CMOS/MEMS Array Microdrop Generator



CFD Analysis of Microdrop Generation

**Coupled Thermal-Fluidic
&
Free-Surface Analysis***

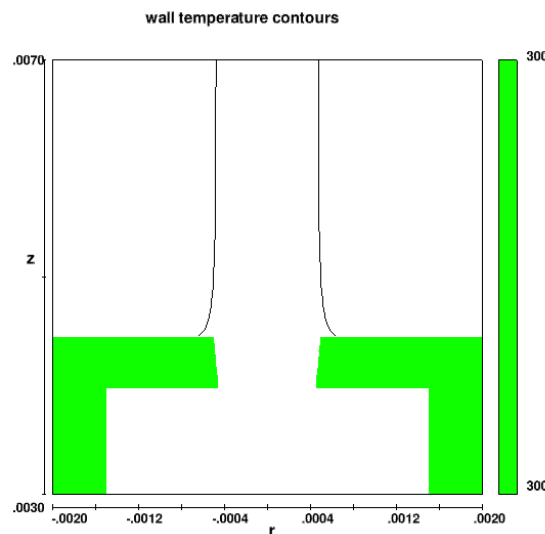
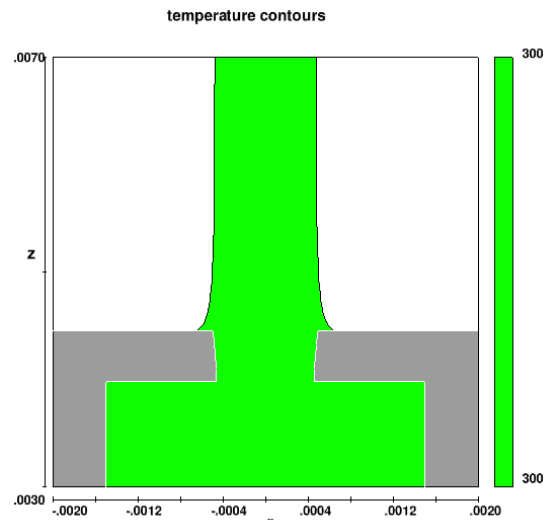
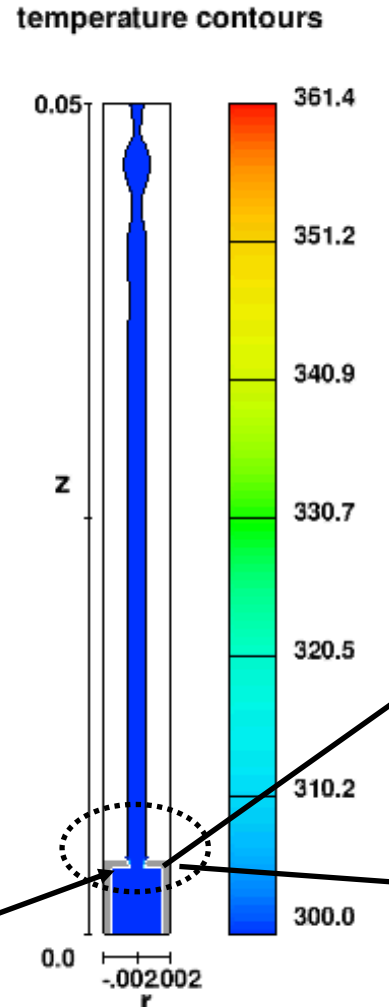
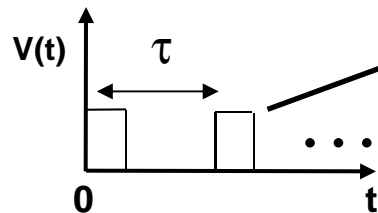
$$\rho \frac{D v}{Dt} = -\nabla p + \mu \nabla^2 v$$

$$\nabla \cdot v = 0$$

$$\rho c_p \frac{DT}{Dt} = k \nabla^2 T$$

Quad-Core Workstation
2.8 GHz Processors
Windows XP 32 Bit
8 GB RAM

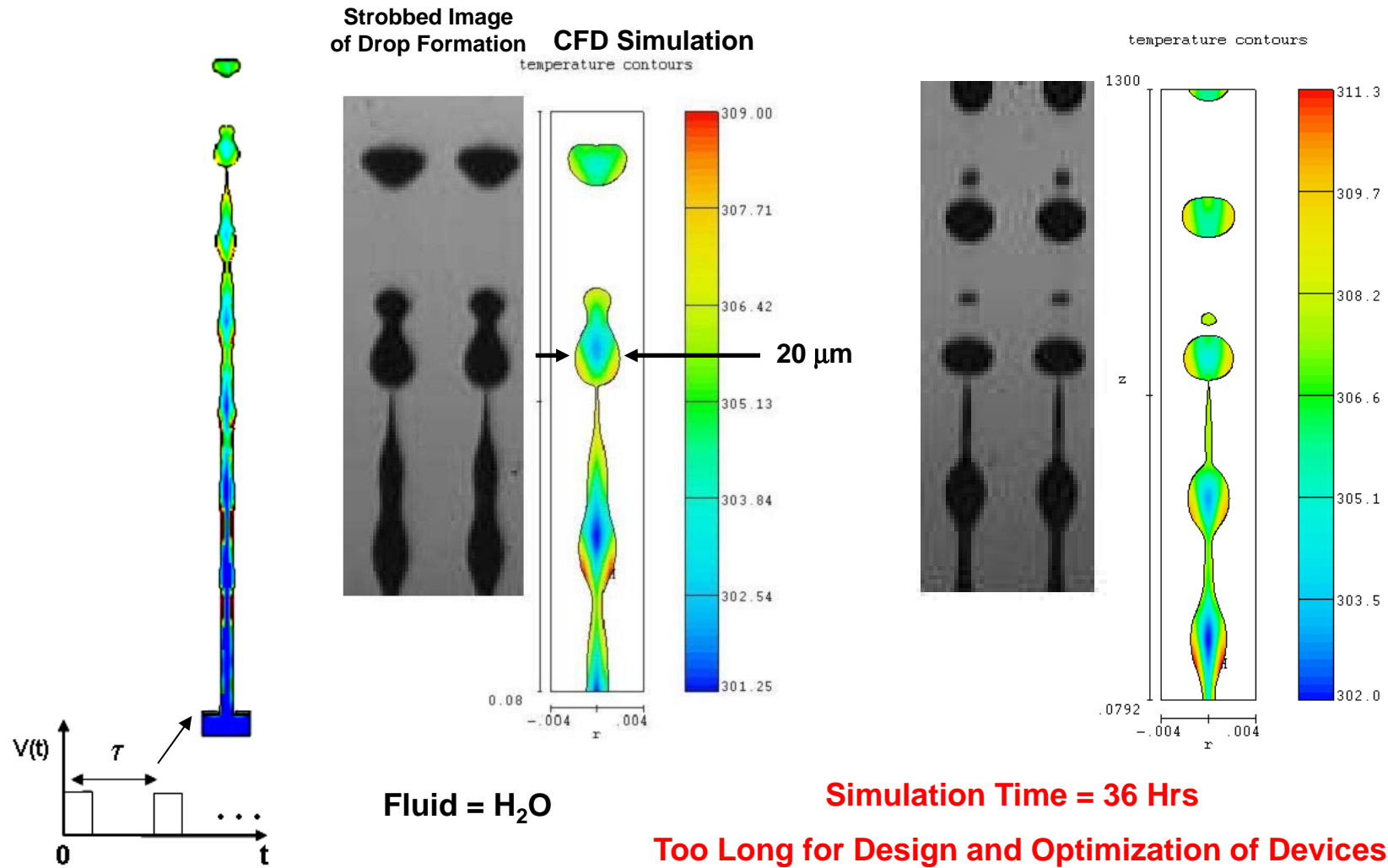
Simulation Time = 36 Hrs



*FLOW 3D - VOF Solver

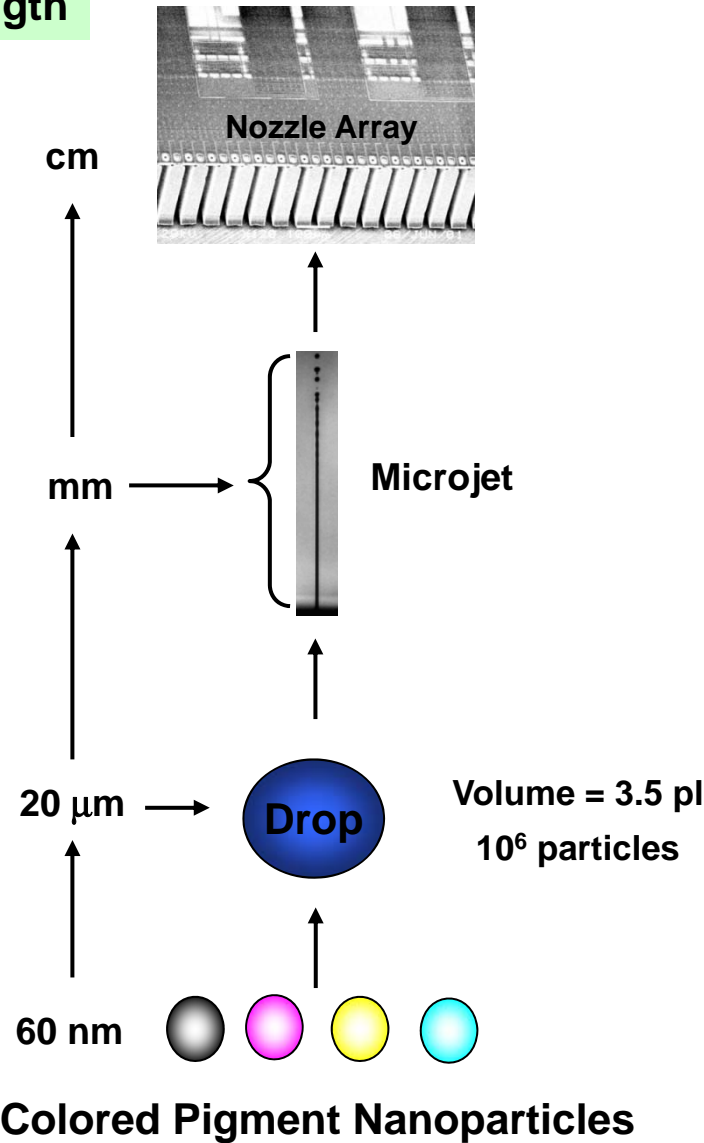
Microdrop Generation: Model vs. Experiment

No Fitting Parameters!

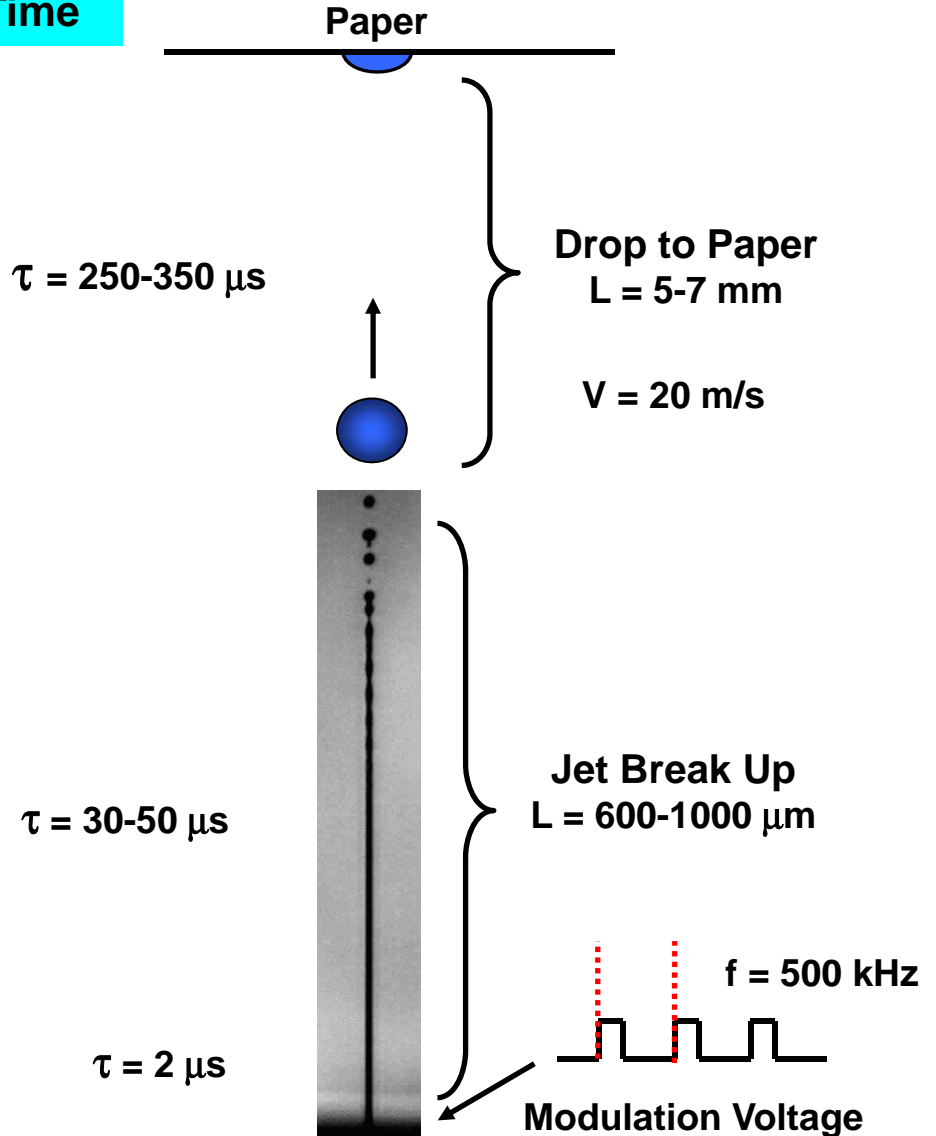


Length and Time Scales

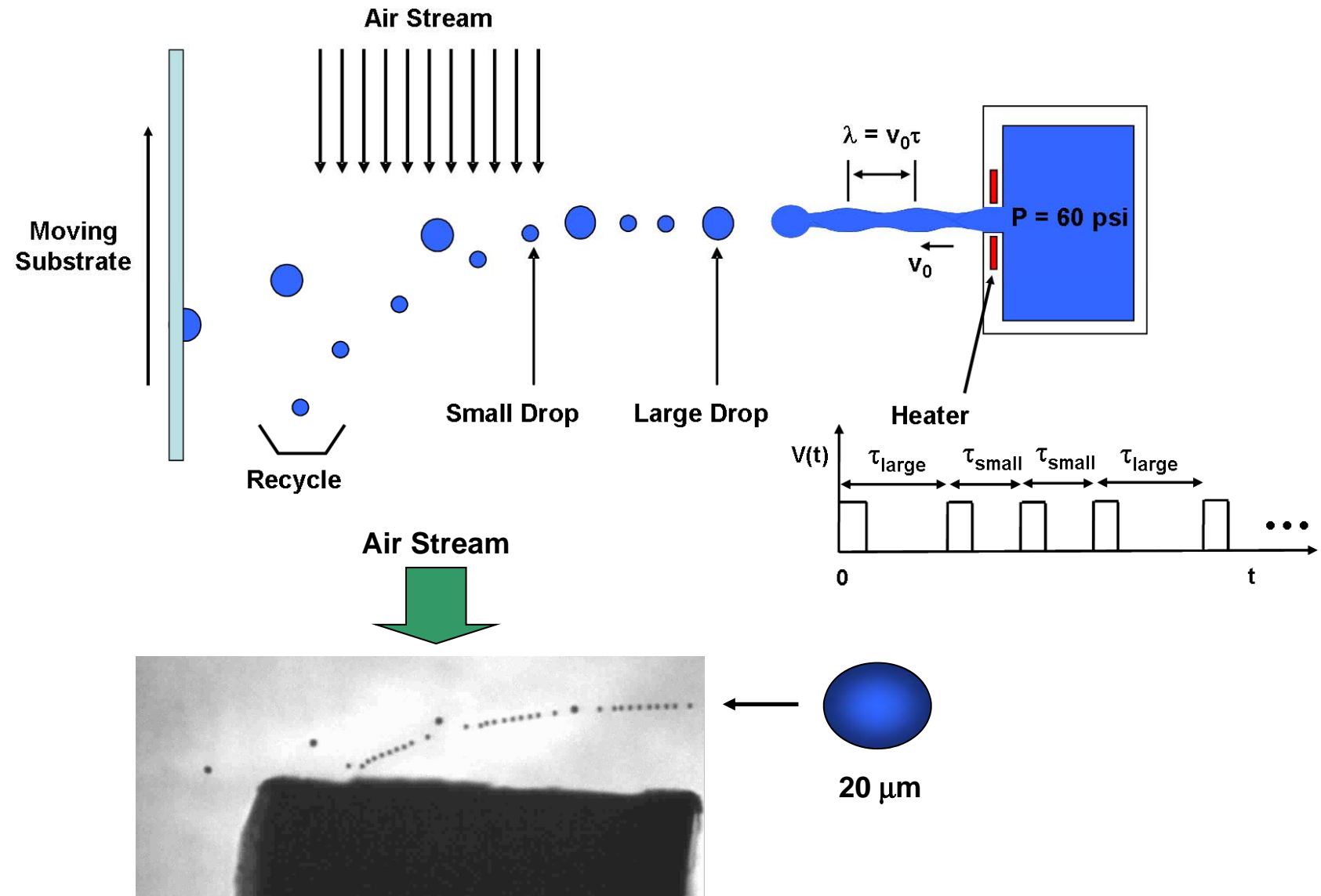
Length



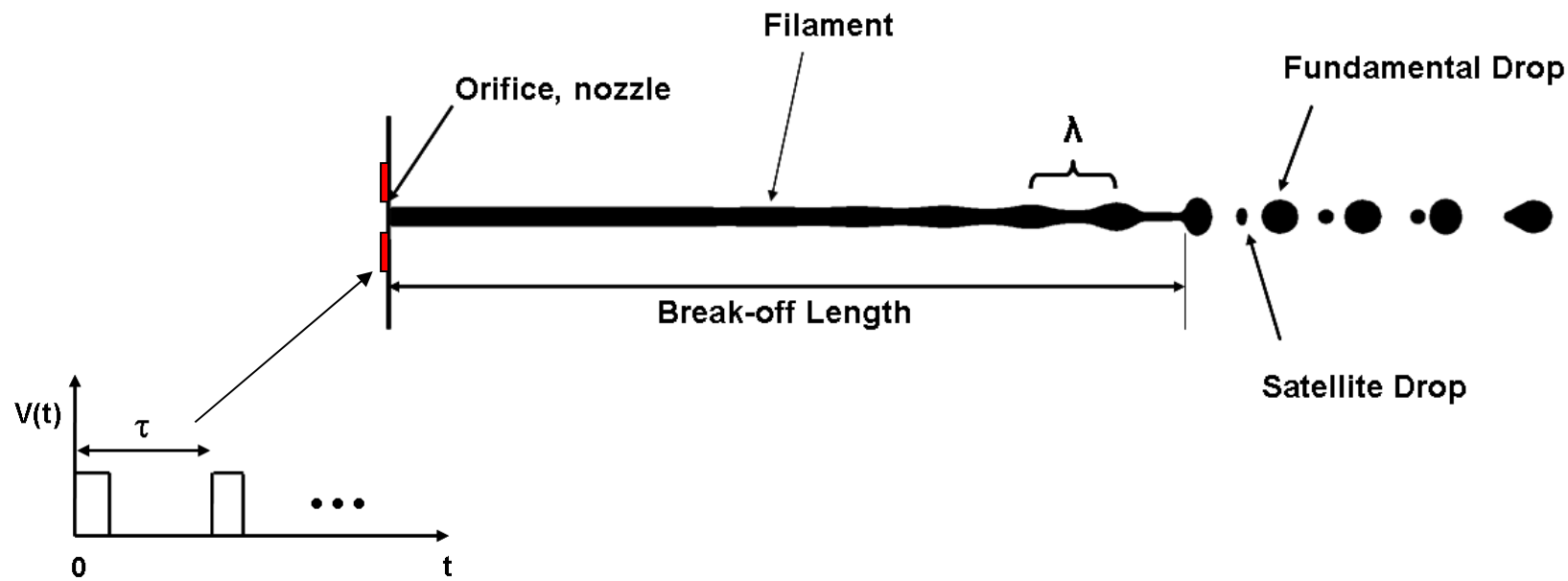
Time



Drop Size Selection - Air Deflection



Performance Optimization



Optimize Voltage Waveform:

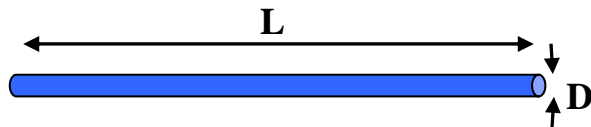
- Control jet Breakup Length
- Control Drop Volume & Velocity
- Maximize Drop Generation Frequency
- Suppress Satellite Drops

CFD Simulation = 36 Hrs
Awkward for Optimization



Slender Jet Analysis
Simulation Time = Minutes

Slender Jet Analysis



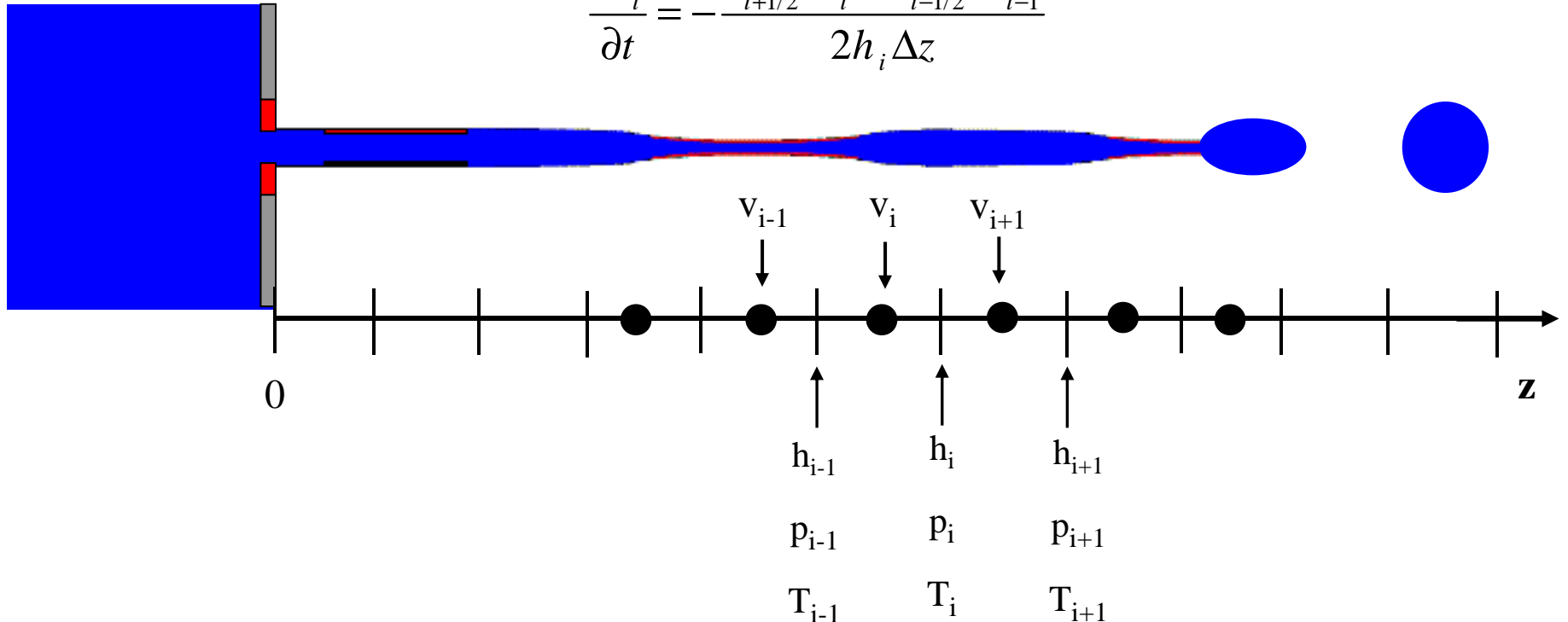
Method of Lines

$$\frac{\partial v_0}{\partial t} + v_0 \frac{\partial v_0}{\partial z} = -\frac{1}{\rho} \frac{\partial(2\sigma H)}{\partial z} + \frac{3\mu}{\rho h^2} \frac{\partial}{\partial z} \left(h^2 \frac{\partial v_0}{\partial z} \right) + \frac{2}{\rho h} \frac{\partial \sigma}{\partial z} + \frac{3}{\rho} \frac{\partial \mu}{\partial z} \frac{\partial v_0}{\partial z}$$

$$\frac{\partial T_0}{\partial t} + v_0 \frac{\partial T_0}{\partial z} = \alpha \frac{1}{h^2} \frac{\partial}{\partial z} \left(h^2 \frac{\partial T_0}{\partial z} \right) - \frac{2\alpha\beta}{h(z,t)k} (T_0 - T_\infty)$$

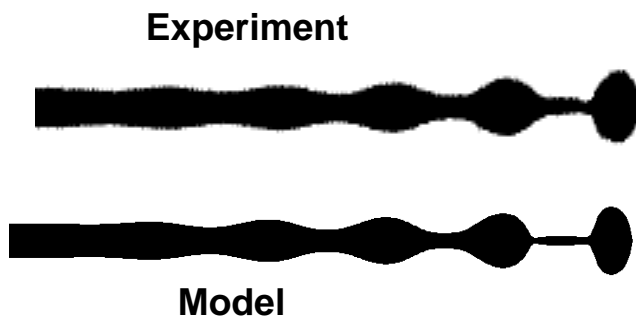
$$\frac{\partial h^2}{\partial t} = -\frac{\partial(h^2 v_0)}{\partial z}$$

$$\frac{\partial h_i}{\partial t} = -\frac{h_{i+1/2}^2 v_i - h_{i-1/2}^2 v_{i-1}}{2h_i \Delta z}$$

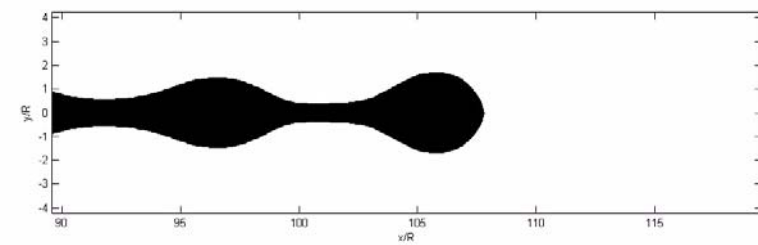
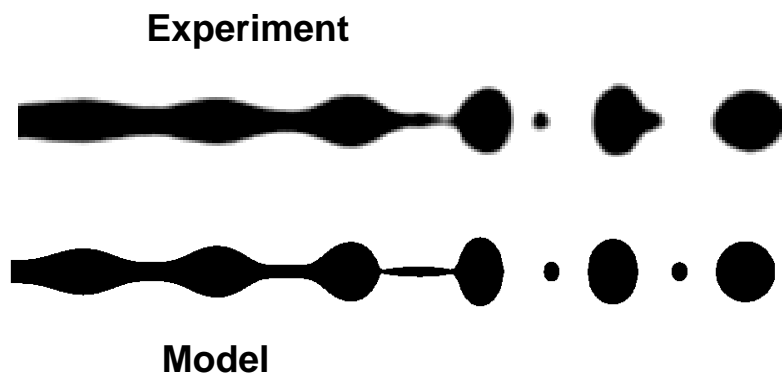
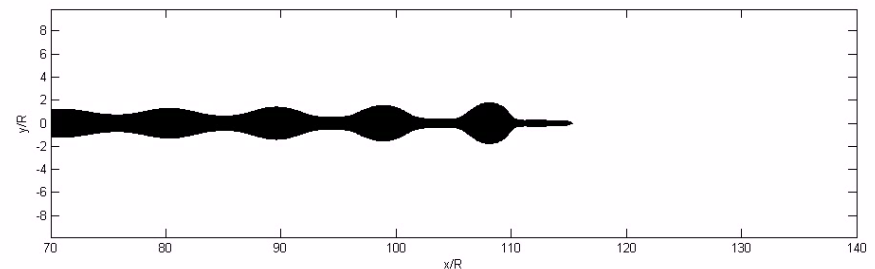


E. P. Furlani and M. S. Hanchak, Nonlinear Analysis of the Deformation and Breakup of Viscous Microjets using the Method of Lines, Int. J. Numerical Methods in Fluids, on line, March 2010.

Slender Jet Analysis vs. Experiment



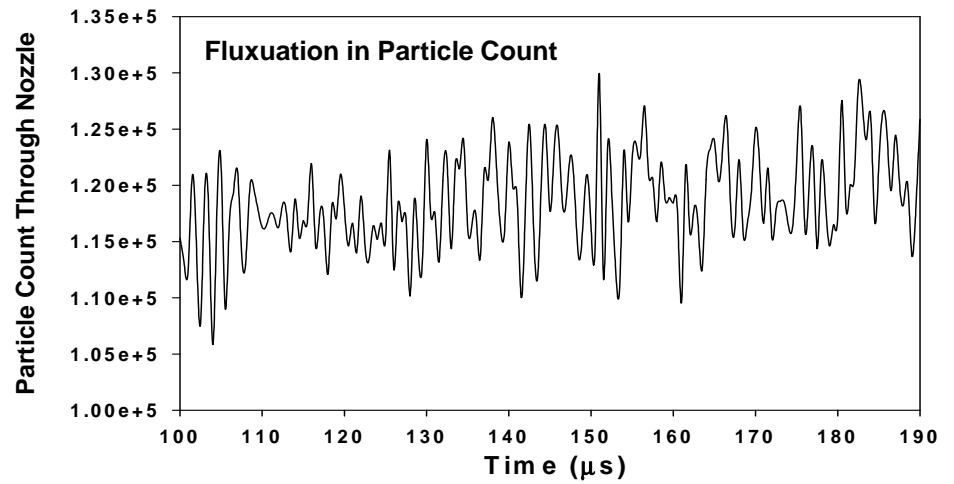
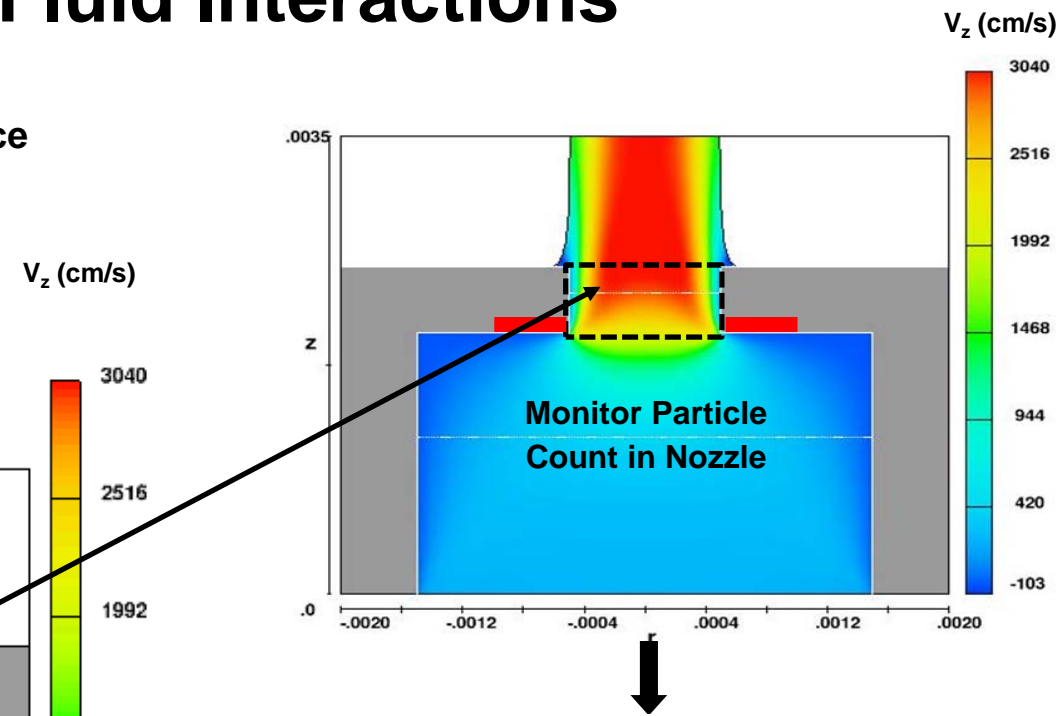
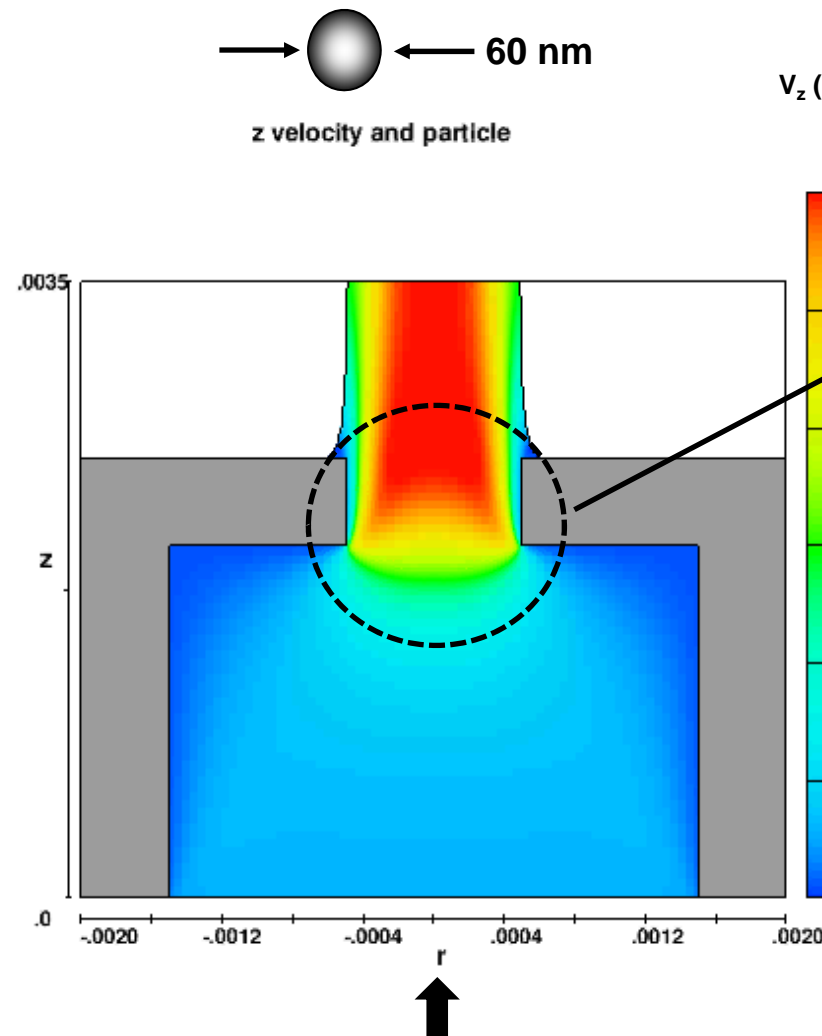
Simulation Time 10-20 min*



*Programmed in Matlab using ODE Solvers

Particle-Fluid Interactions

Flow of Pigment Particles Through Orifice

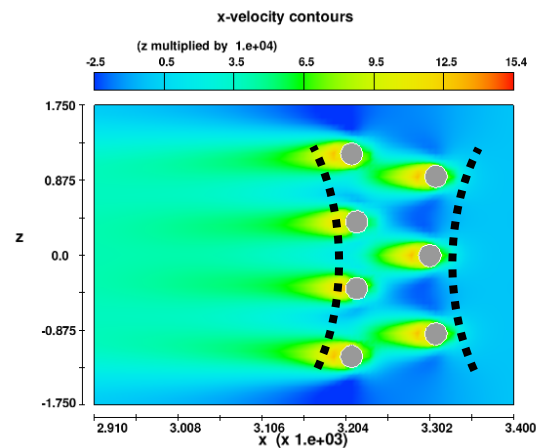
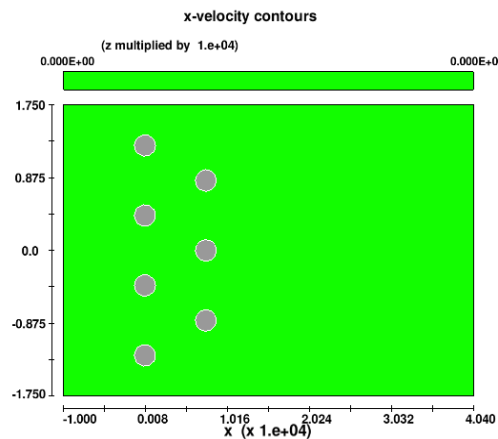
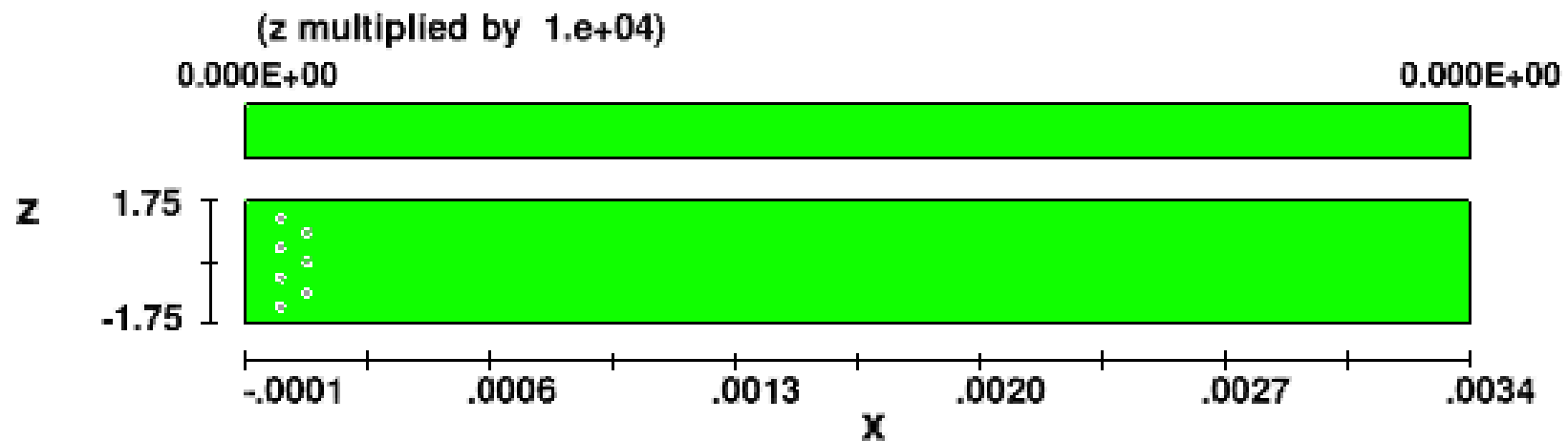


Pigment Nanoparticles

Particle-Fluid Interactions

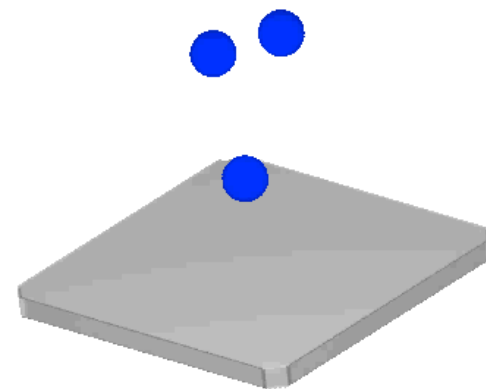
Aerodynamic Droplet Interaction

x-velocity contours



Fluid-Surface Interaction

Coalescence: Multiple Drops Impacting a Surface



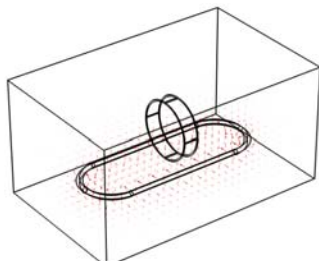
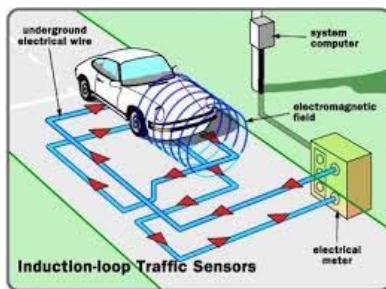
Translational Research

Industrial Grants and Contracts*



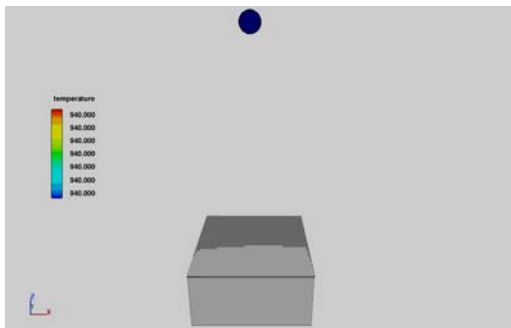
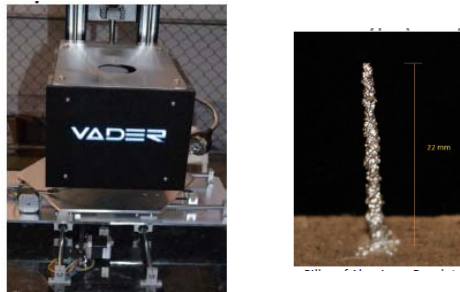
Remote Sensing

2014-2015:
Electromagnetic Modeling
for Development of
Inductive Loop
Technology for
Automobile Sensing



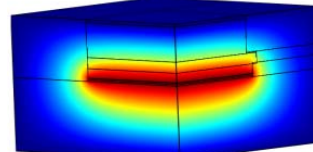
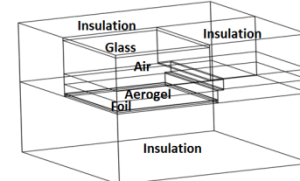
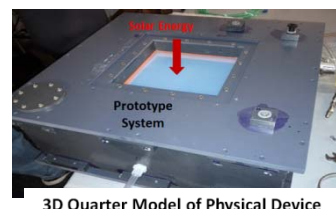
Additive Manufacturing

2014-2015: Multiscale
modeling of
Magnetohydrodynamic-based
Liquid Metal Jet 3D Printing



Energy Harvesting

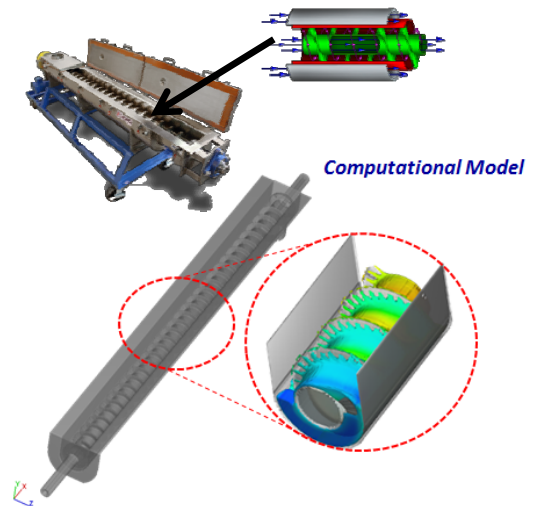
2013-2014: Process and
Materials Modeling involving
Thermal and Gas Dynamics
for Novel Green Energy
Technology based on a
Knudsen Compressor.



Equipment Design

2013-2014: Development of computational fluid dynamic (CFD)-based device and process modeling:

- Design of custom commercial apparatus and processes.
- Coupled heat and mass transfer (flow dynamics) of highly viscous liquid-based, granular and structurally deformable materials.



*Partial support from NYS High Performance Computing Consortium (HPC2)

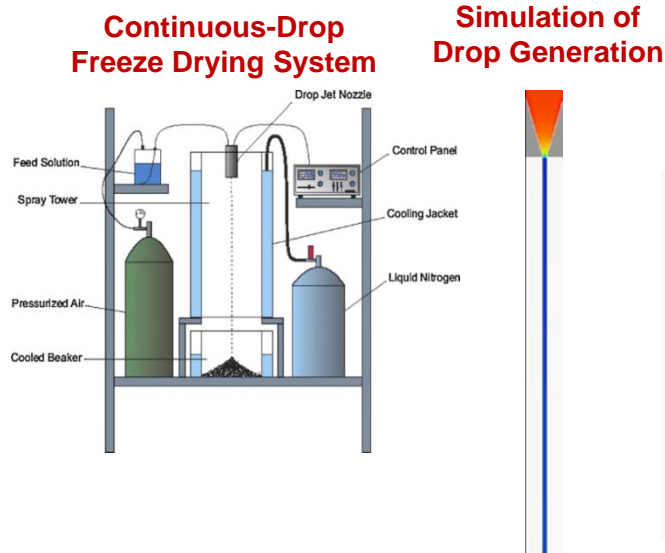
Translational Research

Industrial Grants and Contracts



Pharma

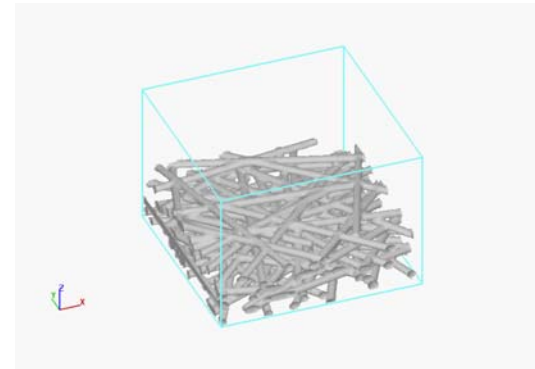
2013: Process and Materials Modeling Involving Thermal/Fluidic/Phase Change Analysis for Novel Commercial Lyophilization (Freeze-Drying) Systems for Pharma Industry.



Nanofluids - Inks

2011-1212: CFD Modeling of Colloidal and Wetting Phenomena in Porous Media for Development of Commercial Pigmented Ink Formulations for Ink Jet Printing

Droplets Impacting Porous Media



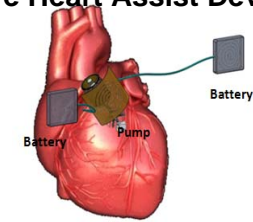
Nanoparticle Synthesis

2011-1212: Thermo/Gas Dynamics Modeling of Chemical Reactor and Reaction Process for Synthesis of Si Nanowires.



CardioVox Biotechnology

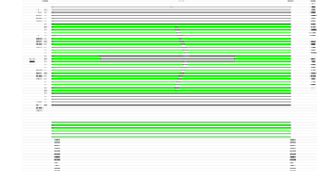
2010-1211: CFD Modeling of Rotary Blood Pump Dynamics and Performance of Aortic Valve Heart Assist Device.



Pump Impeller



Model of Impeller Dynamics



Summary

- 1. Interdisciplinary multiscale modeling is used in industry:**
 - Advance fundamental understanding of new processes, materials and devices
 - Enable rational design and optimization
 - Accelerate development cycle of commercial products
- 2. Significant challenges and opportunities exist for the development of novel algorithms for modeling coupled phenomena across multiple length and time scale.**
- 3. Multicore workstations and high performance computer facilities are becoming more cost effective and accessible for large scale simulations**
- 4. Public domain and commercial software is becoming more available, adaptable and increasingly sophisticated to facilitate analysis.**